

# We are IntechOpen, the world's leading publisher of Open Access books Built by scientists, for scientists

6,900

Open access books available

186,000

International authors and editors

200M

Downloads

Our authors are among the

154

Countries delivered to

TOP 1%

most cited scientists

12.2%

Contributors from top 500 universities



WEB OF SCIENCE™

Selection of our books indexed in the Book Citation Index  
in Web of Science™ Core Collection (BKCI)

Interested in publishing with us?  
Contact [book.department@intechopen.com](mailto:book.department@intechopen.com)

Numbers displayed above are based on latest data collected.  
For more information visit [www.intechopen.com](http://www.intechopen.com)



# Numerical Simulation of Industrial Flows

Hernan Tinoco<sup>1</sup>, Hans Lindqvist<sup>1</sup> and Wiktor Frid<sup>2</sup>

<sup>1</sup>*Forsmarks Kraftgrupp AB,*

<sup>2</sup>*Swedish Radiation Safety Authority  
Sweden*

## 1. Introduction

Computational Fluid Dynamics (CFD) is a numerical methodology for analyzing flow systems that may involve heat transfer, chemical reactions and other related phenomena. This approach employs numerical methods imbedded in algorithms to solve general conservation and constitutive equations together with specific models within a large number of control volumes (cells or elements) into which the associated computational domain of the flow system has been divided to build up a grid.

Numerical simulation of industrial flows using commercial CFD codes is now well developed in a number of technical fields. With the advent of powerful and low-cost computer clusters, events including both complex geometry and high Reynolds numbers, i.e. fully turbulent practical industrial applications, may today be accurately modeled. This technique constitutes a rather new tool for analyzing problems related to, for instance, design, performance, safety and trouble-shooting of industrial systems since time can now be treated fully as the primary independent variable.

The first commercial general-purpose CFD code, built around a finite volume solver, the Parabolic Hyperbolic Or Elliptic Numerical Integration Code Series (PHOENICS), was released in 1981. Initially, the solver was conformed to work only with structured, mono-block, regular Cartesian grids but it was subsequently broadened to admit even structured body-fitted grids. The multi-block grid option was developed many years later within this code which still preserves this restricting structured grid topology. Another well known commercial CFD code, FLUENT, was brought out onto the market in 1983 as a structured software that bore a resemblance to PHOENICS, but aimed towards modeling of systems with chemical reactions, specifically those related to combustion.

Hence, during the 1980s, CFD simulations were limited to rough time-independent models with very simplified geometry due to the grid-structured character of the software and the vast limitations in, at that time, normally available computer resources at the industry (see e.g. Tinoco & Hemström, 1990). It might be of some interest to point out that the top performance of a supercomputer at the end of the 1980s was of the order of 10 GFLOPS ( $10 \times 10^9$  Floating point Operations Per Second). The computers normally available at the industry had a thousandth to a hundredth of that performance, i.e. 10-100 MFLOPS. Today, a computer cluster containing a couple of hundred CPUs has a capacity of the order of TFLOPS.

At the beginning of the 1990s, important steps in software improvement took place through the development of grid-unstructured, parallelized algorithms (e.g. FLUENT UNS) that

enabled the possibility of an accurate geometrical representation of the modeled flow system (see e.g. Tinoco & Einarsson, 1997). At the same time, the communication through adequately formatted geometrical data between grid generators and CAD solid modelers was established and improved. This rather new link allowed the generation of unstructured grids more easily directly from appropriately simplified CAD geometry. However, a new problem arose with the use of CAD models, namely that of “dirty” geometries (see e.g. Beall et al., 2003) caused by relatively large tolerances, leading to gaps and overlaps, and by translating geometries from the native CAD format to another. In the section that follows, the issue of what is meant by grid quality will be assessed from different points of view, including that of the interaction with CAD geometries.

Even if the applications described in the present work have a slight emphasis towards the nuclear power industry, only single-phase phenomena will be discussed in following sections. Two-phase flow simulations are still considered by the authors to have a excessively high level of uncertainty and they have not reached the level of maturity of single-phase simulations. Two-phase phenomena suffer mainly from a deficit of comprehensive knowledge about the physics involved in the different processes included in two-phase flows. Consequently, the models available lack the CFD distinctive prediction capability because they are usually based on information gathered as relatively general correlations. A relevant example of the deficiencies of this field is that nobody has yet succeeded to measure the detailed structure a boundary layer modified by boiling at the wall.

## 2. Grid quality

All geometries to be discussed in this work will be assumed to have been digitally expressed as CAD models, and all CAD models referred to herein are assumed to have been generated by solid modelers. Three-dimensional wireframe and surface models are not an alternative since they do not fulfill the fundamental requirements of an acceptable three-dimensional geometrical model. These models have no volume associated with them and, for instance, the curved surfaces involved have polyhedral approximations that may deteriorate the boundary layer resolution of a grid. A model of a shell may lead to the generation of negative grid volumes since, in this representation, the inner surface may cross the outer surface of the shell due to insufficient resolution of the geometrical model.

The grid is the most basic part of an industrial CFD analysis and reflects nearly all of the aspects to be considered in the flow problem, namely the objective of the analysis, the appropriateness of the geometry and flow domain included, the suitability of the boundaries chosen in connection to properly defined boundary conditions, the space-time resolution needed to cope with the flow characteristics (for instance turbulent, with heat transfer to boundaries, compressible with shocks, with chemical reactions, with two-phases, with free surface, etc.), the need of moving parts to capture the effect of, for instance, rotating pump impellers, closing valves, etc.

### 2.1 Geometrical fidelity, structured grids and multi-block strategy

The absolutely first requirement to be fulfilled by the grid is the high degree of fidelity with which it has to represent the geometry of the flow system. This issue of geometrical fidelity is far from self-evident since, on the one hand, the geometry comprised in a CAD model may contain undersized “intended features” like chamfers and roundings that might need

to be suppressed due to irrelevance for the analysis and/or to grid size limits. On the other hand, the upper size limit for geometrical simplifications is subtle and has to depend on the purpose of the simulation: the elimination of geometrical details must not introduce unwanted flow effects or remove a detectable part of the flow effects to be analyzed.

Prior to the process of grid generation, importing models from a specific CAD platform may either provide too much detail, i.e. the “intended features” mentioned above, or deficient geometric representation with “artifact features” and other incompatibilities, such as the aforementioned gaps and overlaps, that invalidate the model (see e.g. Beall et al., 2003). These deficiencies lead to the problem of “dirty geometries” mentioned before which may nowadays be treated by making small changes to the model through the processes of “healing” gaps, “tweaking” geometries, “defeaturing” unwanted features, “merging” overlapping surfaces, i.e. a “repair” of the geometrical model. Still, this constitutes a rather serious problem for the design/analysis integration in the production line of the manufacturing industry.

The topological character of a structured grid may lead to undesirable oversimplifications of the geometry since it may be extremely difficult or impossible to sufficiently deform the structure of the grid to fit the geometry. A structured grid is laid out in a regular repeating pattern, a block, which accomplishes a mapping defining a transformation from the original curvilinear mesh onto a uniform Cartesian grid, as is shown in Fig. 1 for a two-dimensional case.

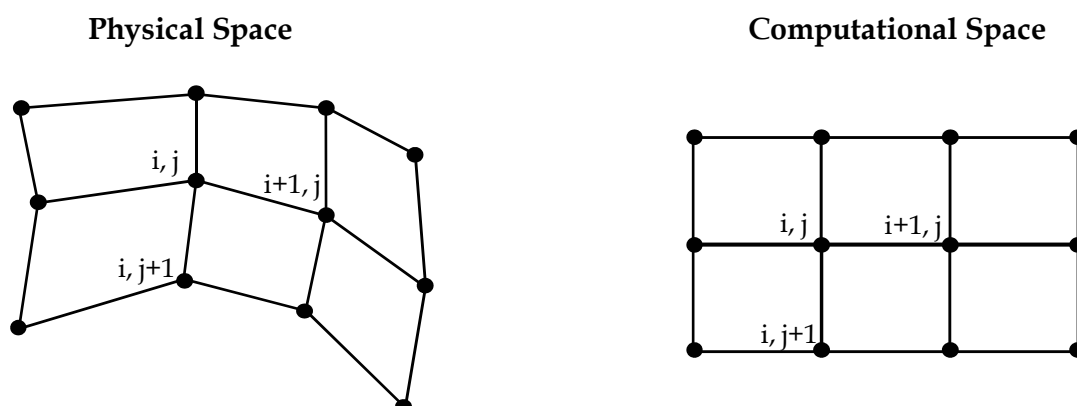


Fig. 1. Mapping associated with a two-dimensional structured grid.

For the pioneering codes of the beginning of the 1980s, this mapping allowed an easy identification of the neighbors of a specific point together with an efficient access to the information pertaining to these neighbors. Also, a complement for rough geometric fitting was available in PHOENICS through porosity, which allowed for a crude representation of curvilinear boundaries using rectangular grids but eliminated the possibility of a proper resolution of the corresponding boundary layer and the near wall flow.

Obviously, the calculations are facilitated by the use of structured grids since less computer resources are needed and the simulation may be speeded up utilizing simpler and more robust algorithms. On the other hand, a local refinement of the grid is impossible since the structure of the grid must be preserved, implying that the inclusion of an extra node results in the addition of a complete line or of a complete plane for, respectively, two- and three-dimensional grids. For instance, if an extra node is located between nodes  $(i, j)$  and  $(i+1, j)$  in the grid of Fig. 1, then a node between nodes  $(i, j+1)$  and  $(i+1, j+1)$  and a further node

between nodes  $(i,j-1)$  and  $(i+1,j-1)$  must be added. If not, the middle row would have one more node than the other rows, destroying by this the structure of the grid.

Another shortcoming of structured grids is their inability of accommodating a single block to a complex geometry such as the one associated with the unstructured surface grid shown in Fig. 2. Here, the geometry corresponds to that of the core shroud (moderator tank), with cover, of a Boiling Water Reactor (BWR). The three-leg pillars that hold the cylindrical drum of the steamdryer support (upper right corner of the view) may be observed at the edge of the cover. In the forefront, the piping of the core spray system and a feedwater sparger has been included in the figure. Steam separators that should have been connected to the outer side of the core shroud cover, have not been displayed in the view of Fig. 2 in order to avoid a forest of cylindrical shaped equipment that would have overloaded the view, rendering it thickly. Only the trace of the connecting circular holes is seen in the core shroud cover.

A strategy to overcome the limitations of a single block structured grid consists of dividing the computational domain in an appropriate number of regions, each one suitable for a single block, i.e. to increase the number of structured grids, one for each block. But now, the difficulties are moved to the issue of connecting the different blocks to build the complete domain. Several block connection methods are available: the point-to-point method, in which the blocks must match topologically and physically at the common boundary, the many-to-one-point method, in which the blocks must match physically at the common boundary, but be only topologically similar, and arbitrary connections, in which the blocks must match physically at the common boundary, but may have significant topological differences. Although the multi-block approach may increase the possibilities of achieving a higher geometrical fidelity of the simulated flow system, the block connection requirements may restrict the quality of the grids, which still are difficult to construct. Also, the price paid by increasing the degrees of freedom in block connectivity is a detriment to the accuracy of the solution and a deterioration in the solver robustness.

## 2.2 Unstructured grids, histogramming and polyhedra

In contrast to the limited possibilities of structured grids, Fig. 2 below constitutes a modest indication of how far it might be possible to get with the requirement of geometrical fidelity if an unstructured grid is used to fit a complex geometry. Unstructured grids lack the mapping of the structured grids and, therefore, the information about the connection of each node between physical space and computational space is kept within the algorithm of the unstructured solver, which has to work out the location of the neighbours of each node, i.e. the node at location "n" in memory may have no physical relation to the node next to it in memory, at location "n+1".

The disadvantages of unstructured grids are the need of larger computer resources and the use of more complex algorithms that may not be as effective as those used with structured grids under similar simulating conditions. Besides the aforementioned degree of geometrical fidelity, unstructured grids have the great advantages of being easily automatized in their generation, requiring limited time and effort in this process, and of readily being suitable for spatial refinement. Depending on the grid generator, a minor drawback with automatization might be the lack of user control when setting up the grid, since most of the user participation may be restricted to disposing the mesh at the boundary surfaces while the interior is automatically filled up by the software. Triangular and tetrahedral elements are not easily deformed, i.e. stretched or twisted, leading to a grid that may be rather isotropic, with elements of roughly the same size and shape. Rather than a

disadvantage, this property may turn out to be of assistance for maintaining almost everywhere in the computational domain a maximum element size of the grid that adequately matches the size of the time step needed for resolving the different structures of the flow to be simulated. Today's possibility of treating the time dependence of the flow with realistic accuracy is undoubtedly having an impact on the perception of grid quality, an subject that will be further discussed in this work.

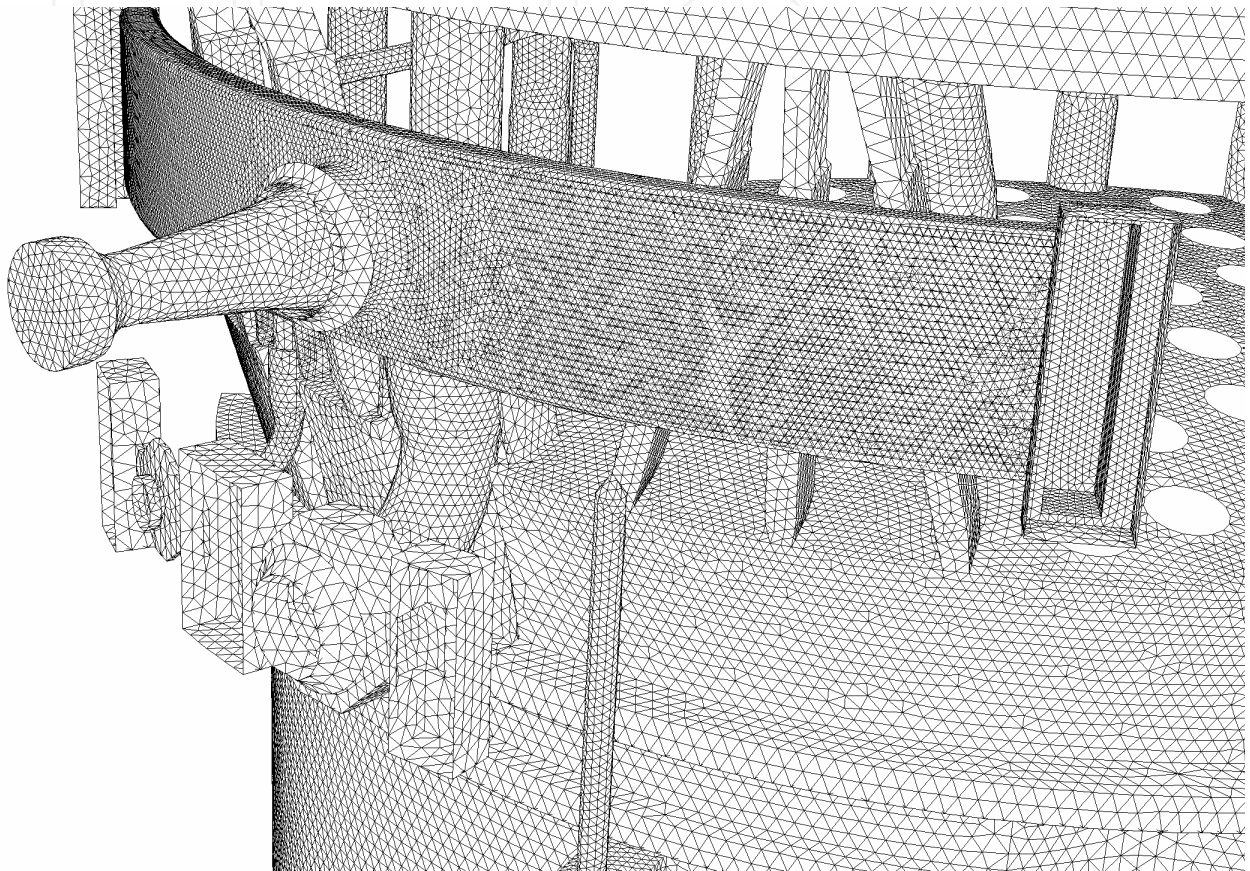


Fig. 2. Unstructured grid of the core shroud and cover of a BWR.

The traditional method for assessing grid quality, giving a statistical measure over the entire computational domain, consists in histogramming (Woodard et al., 1992). Several geometrical parameters are used to evaluate the quality of the individual elements, herein assumed, without losing generality, to be tetrahedra since similar parameter definitions may be obtained for any polyhedron. A few of such parameters are the minimum dihedral angle, the ratio between the areas of the largest and the smallest faces and the volume ratio between the smallest containing sphere and the largest contained sphere of the tetrahedron. The minimum dihedral angle, which is the angle between two planes, is determined by the scalar product of the combination of the four unity normal vectors corresponding to the faces of the tetrahedron. The ratio between areas is found by the combination of the normal vectors to each face obtained through the vector product of two of the three edges making up a face. Although the information provided by these two indicators about the shape of each element is similar, the evaluation of this area ratio is computationally far less demanding than determining the dihedral angles for each face. The aforementioned volume ratio is usually normalized by the value corresponding to a regular tetrahedron, which is

equal to 27 since the ratio of the radii of the spheres is 3. The ratio of the sphere radii, or its inverse value, is generally used as aspect ratios.

Another important parameter for evaluating element quality is skewness, being it a measure of the distortion of the element with respect to an ideal, equilateral element (i.e. regular tetrahedron, cube, etc.). A method to estimate skewness, only valid for tetrahedra, consists of the volume difference between the regular tetrahedron and the actual element shearing the same circumsphere, normalized by the volume of the regular tetrahedron. A more general method for skewness evaluation is the equiangle skew parameter defined by

$$Q_{EAS} = \max \left[ \frac{\theta_{\max} - \theta_e}{180^\circ - \theta_e}, \frac{\theta_e - \theta_{\min}}{\theta_e} \right], \quad (1)$$

where  $\theta_{\max}$  is the largest angle in face or cell,  $\theta_{\min}$  the smallest angle in face or cell and  $\theta_e$  the angle for equiangular face or cell, equal to  $60^\circ$  for tetrahedral and to  $90^\circ$  for hexahedral elements (see e.g. Fluent, 2006). With the above definition, the equiangle skew parameter will range between null and unity, being the maximum skewness value for an acceptable grid not larger than 0.9.

Not only single element quality but also local grid quality needs to be quantified in order to avoid large stretching and/or distorting of the grid. For instance, a doubling in the linear spacing will result in an eightfold increase in volume, leading to large changes in volume ratios. Even if these changes can be detected through analysis of the aforementioned volume parameter, and the grid rectified, the flow structures to be resolved need an even distribution of elements to maintain the accuracy of the simulation, as has already been mentioned. Therefore, a limit in the grid spacing of the order of 10 %, rather than the one normally accepted of about 20 %, should resolve this issue. The grid distortion can be estimated by means of a skewness parameter defined by the ratio between the area of a triangle formed with the center and the two nodes on each side of a chosen face, and the area of the face. If two elements are perfectly aligned, the area of the formed triangle is zero, indicating a local nonexistence of grid skewness.

Grid diagnosis using a methodology of the kind discussed above leads to the necessity of modifying the grid based not only on geometrical criteria but also on concrete physical criteria in order to objectively improve the quality of the grid to be used for the specific flow simulation. As was expressed at the beginning of this section, the grid reflects the simulation problem to be solved and should, consequently, be individual in its quality to conform to the associated physical problem. Therefore, the first, a priori, constructed grid following the aforementioned guidelines will seldom be optimal for the assigned task and will need to be customized through an iterative procedure to comply with the conditions of the physics involved in the simulation. A typical example of this situation is the need for grid refinement in order to capture shocks in aerodynamic applications (see e. g. Borouchaki & Frey, 1998, Acikgoz, 2007). The adaptation is normally achieved using the pressure gradient of the solution as an indicator and, in all probability, the adaptation procedure needs to be repeated several times in order to attain an optimal solution of the grid valid for the specific application.

A particular issue related to grid refinement, which needs special attention due to the connections to other physical phenomena like turbulence and heat transfer, is that of the near wall regions of the flow where large velocity gradients are present, i.e. the boundary layers. In turbulent flows, the wall region is dominated by the effect of shear stress and very

close to the wall, at the viscous sublayer, the scaling parameters are the kinematic viscosity of the fluid and the shear stress at the wall. The characteristic velocity and length scales there are the friction velocity, the square root of the quotient of the shear stress at the wall and the fluid density, and the viscous length scale, the quotient of the kinematic viscosity of the fluid and the friction velocity. Based on these scales, the non-dimensional normal distance to the wall may be expressed in wall units as

$$y^+ = \frac{u_\tau y}{\nu}, \quad (2)$$

where  $y$  is the dimensional normal distance to the wall,  $u_\tau$  the friction velocity and  $\nu$  the kinematic viscosity of the fluid. This distance in wall units is a dynamic measure of the relative importance of viscous and turbulence transport within the boundary layer that affects wall friction, heat transfer, buoyancy and other related physical phenomena. Depending on the degree of approximation of the simulation, a certain minimum value of  $y^+$  is required for the resolution of the computational cells adjacent to the wall in order to capture the correct wall phenomena to the desired level of accuracy.

Further considerations to be presented in the next sections establish that it is turbulence modeling that primarily defines the near wall grid resolution. Additional requirements not only on the normal distance to wall, may however arise due to, for instance, conjugate heat transfer (CHT), natural convection, etc. In the end, the near-wall resolution of the grid is, as the rest of it, solution dependent and has to be optimized by means of refinement through an iterative process.

Finally, some words should be added about the future of grid development. Tetrahedral grids have several already mentioned advantages, but need much larger number of elements for a given volume than grids using other geometrical elements as, for instance, hexahedra, resulting in higher requirements in memory storage and computing time. A tetrahedral control volume has only four neighbors, a property that may deteriorate the computation of gradients in all needed directions. If the neighbor nodes are inadequately located, for example all lying nearly in the same plane, the evaluated gradient normal to that plane may be marred by a large uncertainty. A solution to this and other problems with tetrahedral grids is the use of elements of more complex geometrical shape, i.e. polyhedra (see e.g. Peric, 2004). According to this reference, about four times fewer cells, half the memory and a tenth to a fifth of computing time are needed with polyhedral grids compared to tetrahedral grids for achieving the same level of accuracy of the solution. Two alternatives are now available for generating polyhedral grids, the first to generate the polyhedral grid from scratch and the second to convert tetrahedra to polyhedra from an already existing grid. The later possibility has been tested by the authors with clearly approved result that will be further commented in the next sections (see e.g. Figures 8 and 9).

As will be explained later on, a minimum spatial size of the grid is necessary for a required level of resolution of the turbulent, time dependent structures of the flow, and the feature of polyhedral grids of containing fewer, larger cells may not necessarily be a clear advantage in this kind of simulations. As in every new area of development, more quantitative examination of the properties of polyhedral grids, especially in turbulent, time dependent applications, is needed to get a complete understanding of the virtues of polyhedral elements in industrial simulations.

### 3. Time dependence and turbulence modelling

Time-independent or time-averaged solutions have constituted the traditional methodology of analysing industrial flow applications to obtain fundamental information such as flow direction, pressure drop, mean temperature, etc. Generally, the solutions have been obtained by solving time independent conservation equations, i.e. a steady state approximation, or by a rather short-time average of a rough time dependent solution. Rather often, the time average and steady state solutions of the same flow situation differ, casting a shadow of doubt about the existence and correctness of steady state solutions in industrial flow problems with complex geometries, even as initial guess to time dependent simulations.

As time has passed, the necessity to avoid more and more expensive experimental testing, replacing it by more cost-effective and faster numerical simulations has gradually oriented the CFD activities towards full time-dependent simulations, an evolution brought about mainly by the outstanding development of low-cost microprocessor clusters. Areas like flow induced effects on solid structures, i.e. vibrations, thermal fatigue, cavitation, etc., may now be investigated to a higher level of detail through more comprehensive CFD simulations of the process involved using better suited and more fundamental physical models, i.e. models based on the local flow properties instead of correlation governed global properties. However, this qualitative and quantitative improvement of the CFD analysis tool involves meeting a number of additional conditions, to be discussed throughout the rest of this work, together with a parallel experimental commitment to reinforce and further develop the knowledge about the physical phenomena to be simulated. As already mentioned, this commitment particularly concerns the field of two-phase flows but even issues like unsteady heat transfer to and from a solid boundary needs experimental clarification, as section 4 indicates. In any event, the first and probably rather fundamental condition, concerns the computational grid that now has to comply not only with the general requirements covered in the preceding section but also with those of a more advanced turbulence modelling.

#### 3.1 The numerical solution of the Navier-Stokes equations

The Navier-Stokes equations, describing the motion of Newtonian fluids, are nonlinear partial differential equations that still lack a general, continuously differentiable, analytical solution. Even the issue of the uniqueness of such a general solution has not yet been settled (see e.g. Doering, 2009). Therefore, in order to describe turbulence, which is a time dependent chaotic fluid behaviour, the Navier-Stokes equations are solved numerically through Direct Numerical Simulation (DNS, see e.g. Orszag, 1970) or by first averaging or filtering the equations and solving them numerically together with simpler mathematical models. The first solution approach is extremely time and resource consuming, becoming infeasible for the simulation of industrial flows, for which the only practical solution is to rely on some kind of turbulence model. A large group of models involves resolving of the Reynolds-averaged Navier-Stokes equations (RANS), i.e. a time average of the Navier-Stokes equations, strictly implying that the mean values of the dependent variables are time independent. Assuming that the temporal mean values of the dependent variables may be functions of time, i.e. temporally filtering the Navier-Stokes equations with a filter width which is not infinite but of the order of the turbulent integral timescale, the unsteady terms in the RANS equations are recovered, giving rise to a new group of turbulence models, Unsteady RANS (URANS) models. If the width of the temporal filter is further reduced

towards the Taylor microtimescale and beyond, a complete category of simulation forms, the Partially Resolved Numerical Simulation (PRNS) is obtained (see e.g. Liu & Shih, 2006). In this category, the dependent variables can develop from pure statistical means (RANS) through partially resolved large-scale variables (LES) to, eventually, completely resolved direct-simulated variable (DNS). Of course, depending on the simulation form, a turbulence model appropriate to the filter width must be numerically solved together with the filtered equations in a grid whose resolution is in accordance with the scale content of the resolved field. Figure 3 below shows the energy distribution of a normal turbulence spectrum as a function of the wave numbers in a log-log representation together with the lower scale limits of the resolved spectrum (higher limit of the wave number in light-blue broken lines) for the different groups of turbulence models belonging to the PRNS. In the case of Very Large Eddy Simulations (VLES), to be further discussed in what follows, and Large Eddy Simulations (LES), the limit lies within the inertial sub-range scales of motion where the energy spectrum is a universal function of the wave number, viscosity and dissipation rate (Kolmogorov, 1941, Ishihara et al., 2009).

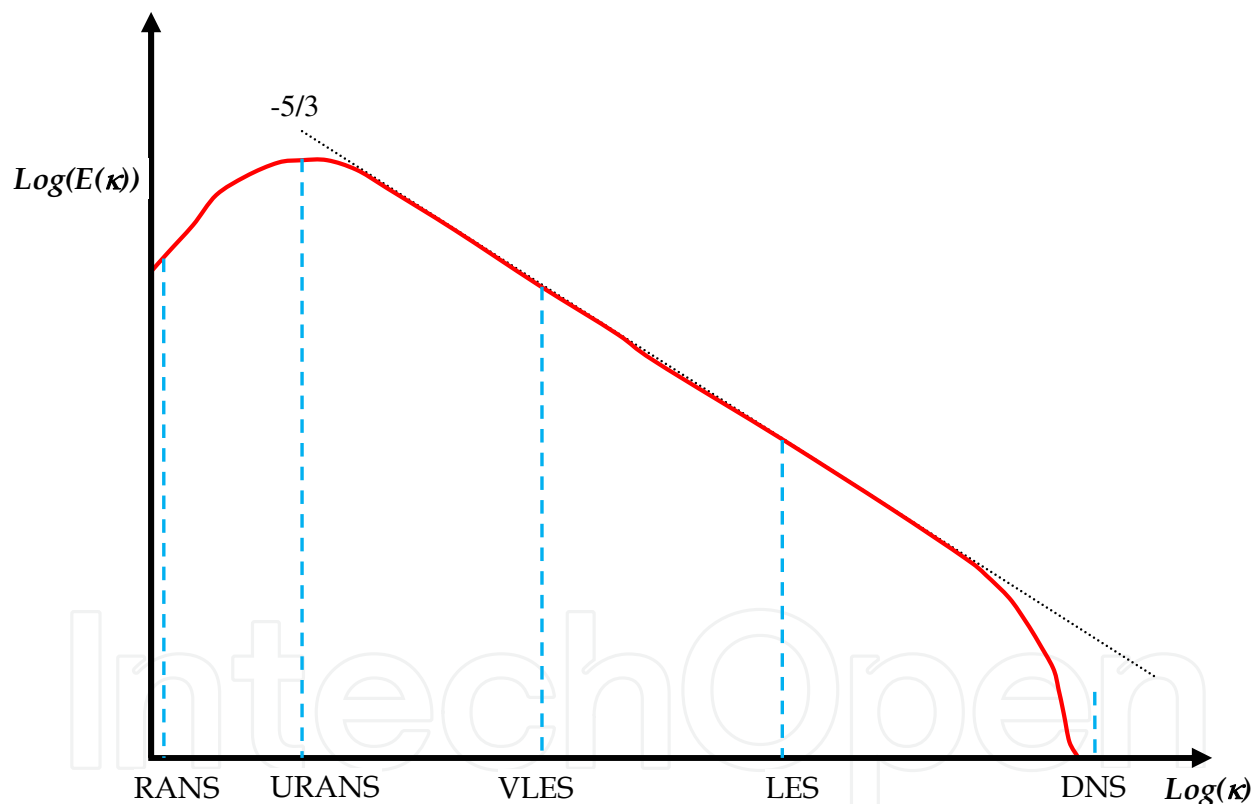


Fig. 3. Schematic view of RANS-DNS resolved energy spectra.

### 3.2 RANS and URANS modeling

RANS turbulence models may be classified by the number of partial differential equations to be solved, namely from zero, i.e. only algebraic equations are solved, through the very popular two-equation models based on the eddy viscosity concept of Boussinesq, like  $k-\varepsilon$  (Jones & Launder, 1973),  $k-\omega$  (Wilcox, 1988) and Shear Stress Transport (SST, Menter, 1994) models, to finally seven equations in the case of the Reynolds Stress Model (RSM, see e.g. Pope, 2000).

Retrieving the time dependent terms through a temporal filter of finite width in the RANS equations allows for time-resolved simulations of turbulent flows together with temporally extended RANS models, in other words URANS models. All empirical parameters and constants in the URANS models maintain the same forms and values as those assigned in the corresponding RANS models.

Time dependent simulations of flows where turbulence effects may be neglected, such as the one generated by a steam-line break in a BWR (Tinoco, 2002), are subjected to less rigorous conditions with respect to space and time resolution. Using a rather coarse grid, of about a few hundred thousand elements, with relatively small time steps may satisfy the Courant number condition ( $Cr < 1$ ) for stable computation of pressure wave propagation without losing too much accuracy. Also, in the case of steam line break, the total simulation time is of the order of some tenths of a second, implying a total number of time steps, about one tenth of a millisecond each, of the order of ten thousand. On the other hand, a turbulent simulation on a grid of many million elements may need a couple of minutes of simulation time, with time steps of the order of a millisecond or less, only for getting rid of the distorting effect of the initial conditions. Even though turbulence-free flow simulations may generate smaller data sets, they might share some problems with turbulent flow simulations in terms of the selection and processing of the data to be saved for further analysis. These issues regard, amongst others, the selection of the adequate variables to be saved for further analysis, the space locations where the variables have to be sampled, the specific views and the figures to choose for a visualization, etc. If the analysis concerns trouble-shooting, a new design or research, the simulation is probably run for the first time, with no or very limited information about the features of the flow to be simulated. Due to storage capacity, it is seldom possible to save a complete data set produced in a simulation of the type mentioned before. Hence, the data to be saved through scripts, to reduce their amount, may have to be defined iteratively since the data selection process depends on the simulation results but should be completed before running the full simulation. Furthermore, the subsequent analysis of the data as, for instance, time series, digital images, etc., is far from trivial and the issue will be further discussed in the rest of this chapter.

Time dependent turbulent flow simulations using URANS may give rather accurate results depending on the turbulence model, the grid resolution and the characteristics of the flow. In this chapter, the analysis of the behaviour of URANS models in time dependent simulations will be mainly concentrated to two-equation models and, in particular, to the SST model of turbulence, due to the rather convincing agreement between results and validation measurements experienced by the authors.

According to Menter (1994), the SST model is a zonal combination of the  $k-\varepsilon$  and  $k-\omega$  models. In contrast to the traditional concept (see Kline, 1989), zonal modelling means here that different models are employed in different regions, using “smart” functions for shifting between models, without the need of a prior knowledge of the flowfield for defining the boundaries for each model. According to this broader definition, model combinations ranging from wall functions and URANS models to Detached Eddy Simulations (DES), to be discussed later in this chapter, may be interpreted as zonal modelling.

The free stream constituent of the SST model, the  $k-\varepsilon$  model, solves one transport equation for the turbulent kinetic energy,  $k$ , and one for the energy dissipation rate,  $\varepsilon$ . It is one of the most widely used two-equation models and has been especially successful in modelling flows with strong shear stress. However, this model has a number of well known shortcomings, notably its lack of ability to correctly predict flow separation under adverse

pressure gradients together with the numerical stiffness of the damping-function-modified equations when integrated through the viscous sublayer. An accurate and robust alternative for dealing with the aforementioned limitations is the  $k-\omega$  model that solves instead a transport equation for the specific energy dissipation rate (or turbulent frequency)  $\omega$ . This model behaves significantly better under adverse pressure-gradient conditions and has a very simple formulation in the viscous sublayer, without damping functions and with unambiguous Dirichlet boundary conditions. Yet, this model has an important weakness with respect to non-turbulent free-stream boundaries, such as in a jet discharged to a quiescent environment: an unphysical, non-zero boundary condition on  $\omega$  is required and the computed flow strongly depends on the value specified. To take advantage of both models, the SST model solves the  $k-\omega$  model in the near wall region and the  $k-\varepsilon$  model in the bulk flow, coupled together through a blending function that ensures a smooth transition between the models.

After approximately ten years from its birth, a first review of a slightly modified model, was conducted by Menter et al. (2003), in which its strengths and weaknesses when applied to industrial problems, mostly connected to aeronautical issues, were discussed and analysed mainly within the context of time independent solutions. However, the time dependent hybrid DES formulation of Spalart et al. (1997), based on combination of the RANS-SST model and a LES formulation, was also examined due to its improved prediction capabilities, especially in unsteady flow with separation, but also due to one of the shortcomings of the method, i.e. premature grid-induced separation caused by grid refinement. DES, which is one of the alternatives for dealing with unsteady flow situations that cannot afford a proper LES requiring, for instance, a detailed resolution of the boundary layers, has been newly reviewed by Spalart (2009) and will be briefly discussed farther on.

Last year, a second review of the SST model, even this with industrial implications, was completed by Menter (2009), with a stronger accentuation on time dependent simulations. Also the SST model sensitized to unsteadiness through the Scale Adapted Simulation (SAS) approach (Menter et al., 2003, Menter & Egorov, 2004, Menter and Egorov, 2005), i.e. the SST-SAS model of turbulence, is examined and discussed. Some results obtained with the model are compared with both unsteady results obtained with the traditional SST model (SST-URANS) and results obtained with LES. The conclusion that may be drawn from these comparisons is that the spectrum of resolved scales produced in a SST-SAS simulation is broader than that in a URANS simulation but narrower than the corresponding in a LES, i.e. a SST-SAS simulation is equivalent to a VLES.

Over the years, the SST model has become one of the most popular two-equation models of turbulence, and a quite large number of time dependent simulations have been already reported in the literature. Some of the applications consist of cases with a rather academic emphasis, like the work of Davidson (2006) comparing the SST model with its VLES modification, the SST-SAS, in channel flow, in the flow through an asymmetric diffuser and in the flow over and around an axi-symmetric hill. As Davidson points out, URANS models are well dissipative, implying that they are not easily triggered into unsteady mode unless the flow instabilities are strong, like in vortex shedding behind bluff bodies (see e.g. Young & Ooi, 2004, Kim et al. 2005) or in high-Reynolds number jet flow (Tinoco & Lindqvist, 2009, Tinoco et al., 2010), and/or the mesh is fine enough to rule out steady solutions. This paper confirms the aforementioned conclusion about the behavior of the SST-SAS model of producing a simulation similar to VLES but, in some cases, like in the asymmetric diffuser, it may result in a poorer solution and, in some other cases, like in the axi-symmetric hill, it

may behave as poorly as the SST model. These results indicate that the SST-SAS model may not unambiguously tend to improve a URANS simulation by increasing the resolved scales and by, in this sense, approaching a LES since the additional terms, other parts of the model and/or a combination of both may obstruct a sound behavior. A further corroboration of a probable defective behavior of the SST-SAS model consists of its poor performance when used for modeling the OECD/NEA-Vattenfall T-junction Benchmark Exercise (see OECD, 2010, Mahaffy, 2010). A simpler and more straightforward approach to VLES based on the SST model, which incidentally performs rather well in the abovementioned exercise, will be presented, discussed and evaluated in this section.

Before leaving the general discussion about URANS, and the assessment of the SST model in particular, it may be of some interest to name some of its reported applications. Among those with a more academic taste, it is possible to list the following: synthetic jet flow (Rumsey, 2004, Vatsa & Turkel, 2004, King & Jagannatha, 2009), cavity flow (Hamed et al., 2003), base flow (Forsythe et al., 2002), bluff body flow (Young & Ooi, 2004, Kim et al. 2005, Uffinger et al., 2010), wave-maker flow (Lal & Elangovan, 2008), tip vortex flow (Duraiamy & Iaccarino, 2005), flow over airfoils and a turbine vane (Zaki et al., 2010). Also more complex problems, especially concerning the geometry and/or the modeling, have been tackled using the SST model of turbulence, such as fire flow in enclosures (Zhai et al., 2007), flow in a stirred tank (Hartmann et al. 2004), the cooling flow within a divertor magnetic coil of the fusion reactor ITER (Encheva et al., 2007), the flow around seabed structures (Hauteclocque et al., 2007), the flow in a centrifugal compressor stage (Smirnov et al., 2007) and the flow in nuclear reactors (Tinoco & Ahlinder, 2009, Tinoco & Lindqvist, 2009, Tinoco et al., 2010, Höhne et al. 2010). However, only few cases among the aforementioned examples have grids fine enough to overcome the dissipative character of the URANS approach and resolve details of the turbulent flow (Rumsey, 2004, Tinoco & Lindqvist, 2009, Tinoco et al., 2010). In spite of the large number of cells used in some cases, as in Tinoco & Ahlinder (2009) where more than 25 million cells are employed for the reactor model, the behavior of the flow is still inherently steady.

### 3.3 LES, DES and VLES

The evolution towards unsteady simulations in CFD has not been driven by a pure academic interest but rather by a concrete requirement in industrial simulations of finding the correct solution to troublesome problems. The paradigm of this kind of problems is the flow in a tee-junction connecting two pipes of, in general, different diameters with different flow rates and temperatures (see e.g. OECD, 2010). Figure 4 below shows a view along a longitudinal, vertical, central plane of the instantaneous temperature distribution obtained through a time dependent CFD simulation using a high quality grid with 11 million cells but with a rather low Reynolds number of about  $8 \times 10^3$ . This solution, which happens to be identical to its temporal mean value since the turbulence model performs in steady mode, does not allow for an analysis of the risk for thermal fatigue of the pipe wall since no temperature fluctuations are resolved. This case has shown to be ideal for LES, or to be precise DES, since simulations with coarse grids, containing as few as  $3 \times 10^5$  cells (see OECD, 2010), may deliver relevant information of the resolved flow away from the walls (see Fig. 6). To properly resolve the wall regions, including for this case the relevant effect of CHT, the grid requirements for LES increase explosively, with limits not only for the normal dimensions of the cells adjacent to the wall,  $y^+ \leq 1$ , but also for streamwise dimensions,

$x^+ \leq \sim 20$ , and for the spanwise dimensions,  $z^+ \leq \sim 10$  (see Veber & Carlsson, 2010). Moreover, if the value of the Reynolds number corresponds to what is normal in industrial applications, i.e. of the order of million, the computational resources needed may become insurmountable (see e.g. Spalart, 2009).

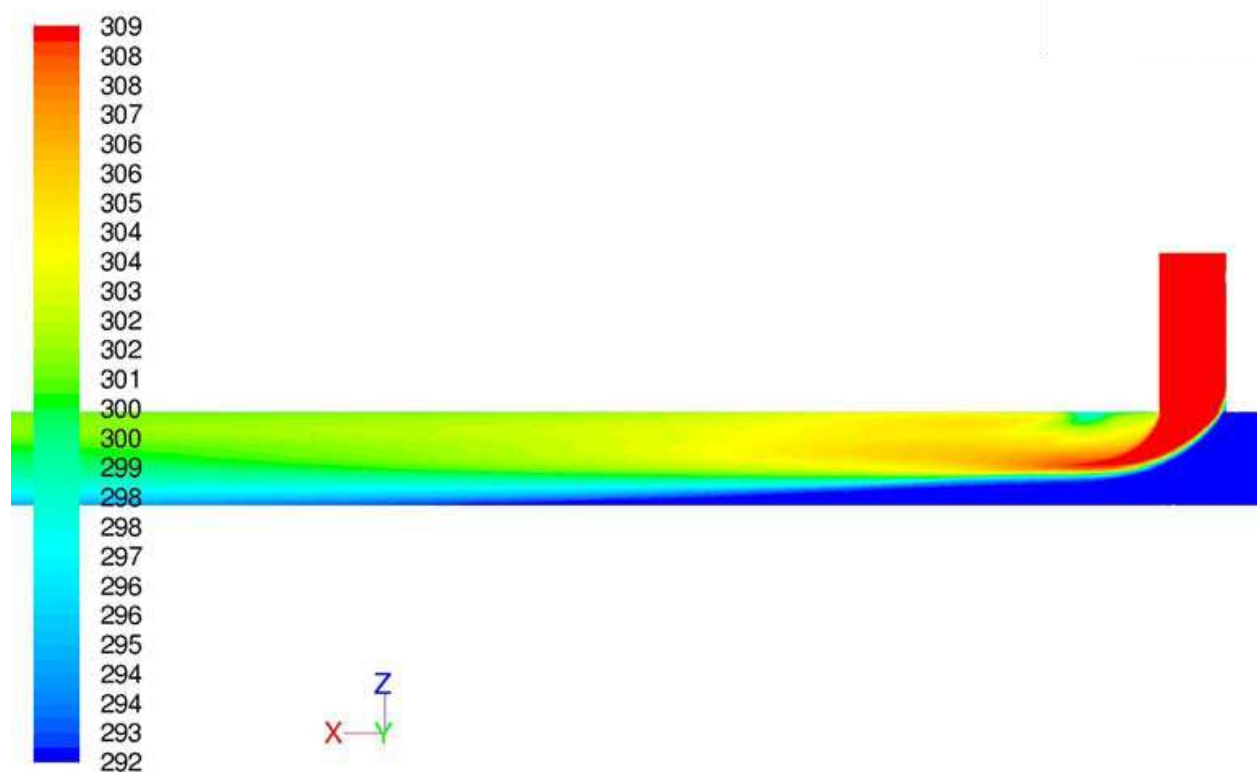


Fig. 4. SST solution of the instantaneous temperature distribution (K) along a longitudinal, vertical, central plane bisecting a tee-junction.

The preceding illustration about the need for unsteady analysis of industrial problems motivates a search for other less demanding alternatives to deal with the problems exemplified by the tee-junction. An option already mentioned in connection with zonal modeling is constituted by DES, which may be based on a combination of LES and URANS (see Spalart, 2009) but may also involve LES and simpler wall-modeling strategies like wall functions. The development of DES has been impelled by the belief that, separately, LES and URANS are incapable of solving the problems discussed above. This is a fact with modification since, as the rest of this section intends to show, a for VLES adjusted URANS may become the sought alternative for unsteady analysis of industrial problems. Different DES formulations using the SST model as the RANS component (Spalart, 1997, Morton et al., 2004, Li, 2007, Lynch & Smith, 2008, Gilling et al., 2009, Dietiker & Hoffmann, 2009, Zaki et al., 2010) have been applied to a wide variety of problems, again with an emphasis on aerodynamics, giving encouraging results. In any event, DES still demands significant computer and software resources and, at the same time, suffers from a number of pitfalls like the already mentioned premature grid-induced separation (Menter et al., 2003) and the more serious difficulties to demonstrate grid convergence and the absence of a theoretical order of accuracy (Spalart, 2009) together with the log-layer mismatch in channel flow simulation (Hamba, 2009). For instance, DES simulations

of the same case reported in the RANS simulations of Tinoco & Lindqvist (2009) and Tinoco et al. (2010), but with a 360° model containing slightly more than 70 million cells (see Veber, 2009), was run continuously during three month in a 256 Intel Xeon CPU machine and reached a simulation time of approximately one minute. An analysis of the temperature signals of some individual points showed temporal means that were not well converged, indicating that the computations would probably need to double the simulation time to reach the same level of convergence as that of the RANS simulations.

The Partially Resolved Numerical Simulation (PRNS) approach has been suggested by Liu & Shih (2006) and is motivated by the assertion that small-scale motions have small associated time scales, allowing for the use of temporal filtering for defining the resolved scales (see also Shih & Liu 2006, Shih & Liu, 2008, Shih & Liu 2009 and Shih & Liu, 2010). Other methodologies for achieving PRNS, not necessarily relying on temporal filtering, have been proposed in the literature, such as that of Ruprecht et al. (2003), that of Perot & Gadebusch (2007, 2009) or the one of Hsieh et al. (2010), but the abovementioned approach of Liu & Shih is the most attractive due to its inherent simplicity. Temporal filtering has been demonstrated by Fadai-Ghotbi et al. (2010) to offer a consistent formalism for a broad class of modeling methodologies that seamlessly unifies a URANS behavior of the simulation in some regions of the flow, e.g. wall regions, with a LES behavior in other regions where explicit resolution of large-scale structures is required. It is also concluded in this reference that the category of models that ranges from RANS to LES may be regarded as temporal filtered approaches depending on a filter width that needs not to be addressed explicitly. In the brief review of the approach of Liu & Shih (2006) that follows, the large-scale motions are defined using a temporal filter of fixed width, i.e. if  $\phi$  is a large-scale variable then

$$\bar{\phi}(t, x_i) = \int_{t-\Delta T/2}^{t+\Delta T/2} \phi(t', x_i) G(t-t') dt', \quad (3)$$

where  $G(t-t')$  is a normalized homogeneous temporal filter. The following top hat filter corresponds to this type of filter, i.e.

$$G(t-t') = \begin{cases} \frac{1}{\Delta T}, & \text{if } |t-t'| \leq \frac{\Delta T}{2} \\ 0, & \text{otherwise} \end{cases}, \quad \text{with } \int_{-\infty}^{\infty} G(t-t') dt' = 1. \quad (4)$$

Performing the filtering operation defined by Equation (3) on the Navier-Stokes and mass conservation equations, a set of exact equations for resolved, large-scale turbulence ( $\bar{\phi}$ ) is obtained

$$\begin{aligned} \rho_{,t} + (\rho \bar{u}_i)_{,j} &= 0, \\ (\rho \bar{u}_i)_{,t} + (\rho \bar{u}_i \bar{u}_j)_{,j} &= \bar{p}_{,i} - \tau_{ij,j} + 2\mu \left( \bar{S}_{ij} - \frac{1}{3} \delta_{ij} \bar{S}_{kk} \right)_{,j}. \end{aligned} \quad (5)$$

In these equations the notations “ $t$ ” and “ $j$ ” denote temporal and spatial derivatives, respectively,  $\rho$ ,  $u_i$ ,  $p$ ,  $\mu$ , are, respectively, density, velocity, pressure and dynamic viscosity, and  $S_{ij} = (u_{i,j} + u_{j,i})/2$  is the rate of strain tensor. The extra unknown term  $\tau_{ij}$  corresponds to the subscale stresses that have to be modelled in order to close the system of equations in

(5). In this case, Boussinesq's eddy viscosity concept will be adopted as the modelling approach, i.e.

$$\tau_{ij} = -2\mu_T \left( \bar{S}_{ij} - \frac{1}{3} \delta_{ij} \bar{S}_{kk} \right) + \frac{1}{3} \delta_{ij} \tau_{kk}, \quad (6)$$

where  $\mu_T$  is the turbulent eddy viscosity. The definition of turbulent viscosity corresponds to that of the SST model, a definition that involves  $k$ , the turbulent kinetic energy and  $\omega$ , the specific energy dissipation rate, implying that two additional equations (see e.g. ANSYS Fluent, 2006) are needed for completing the model characterization. The definition of the turbulent viscosity belonging to the SST model, including the VLES modification according to Liu & Shih (2006) that corresponds to the addition of a factor, the Resolution Control Parameter ( $RCP \leq 1$ ), is

$$\mu_t = (RCP) \frac{\rho k}{\omega} \frac{1}{\max\left(\frac{1}{\alpha^*}, \frac{SF_2}{a_1 \omega}\right)}, \quad (7)$$

where  $S \equiv (2S_{ij}S_{ij})^{1/2}$  is the strain rate magnitude,  $y$  the distance to the nearest wall and

$$\begin{aligned} F_2 &= \tanh(\Phi_2^2), \\ \Phi_2 &= \max\left(\frac{2\sqrt{k}}{0.09\omega y}, \frac{500\mu}{\rho y^2 \omega}\right), \\ \alpha^* &= \alpha_\infty^* \frac{\left(\alpha_0^* + \frac{Re_t}{R_k}\right)}{\left(1 + \frac{Re_t}{R_k}\right)}, \\ Re_t &= \frac{\rho k}{\mu \omega}, \\ \alpha_0^* &= \frac{\beta_i}{3}. \end{aligned} \quad (8)$$

The different constants in the expressions above adopt the following values:  $\alpha_\infty^* = 1$ ,  $R_k = 6$ ,  $a_1 = 0.31$  and  $\beta_i = 0.072$ .

The new factor,  $RCP$ , in the definition of the turbulent viscosity is defined as the ratio of two time scales, namely the filter width,  $\Delta_T$ , and the global turbulent time integral scale,  $T$ . According to the analysis of Liu & Shih (2006), an estimate of the lower limit of  $RCP$  may be obtained using instead a quotient of length scales, an equivalence supported by the study of Fadai-Ghotbi et al. (2010), giving in this case

$$RCP \geq (\Delta/\ell)^{4/3}, \quad (9)$$

where  $\Delta$  is the typical grid size and  $\ell$  is the turbulent integral length scale estimated through (see e.g. Wilcox, 1994)

$$\ell = \frac{\sqrt{k_{URANS}}}{\omega_{URANS}}, \quad (10)$$

where the index “URANS” means the typical values of the corresponding magnitudes obtained with a pure URANS simulation, i.e.  $RCP \equiv 1$ . In addition, the applications to be reported in what follows has been simulated assuming that the SST model of turbulence does not need to be modified when used together with the VLES approach<sup>1</sup>.

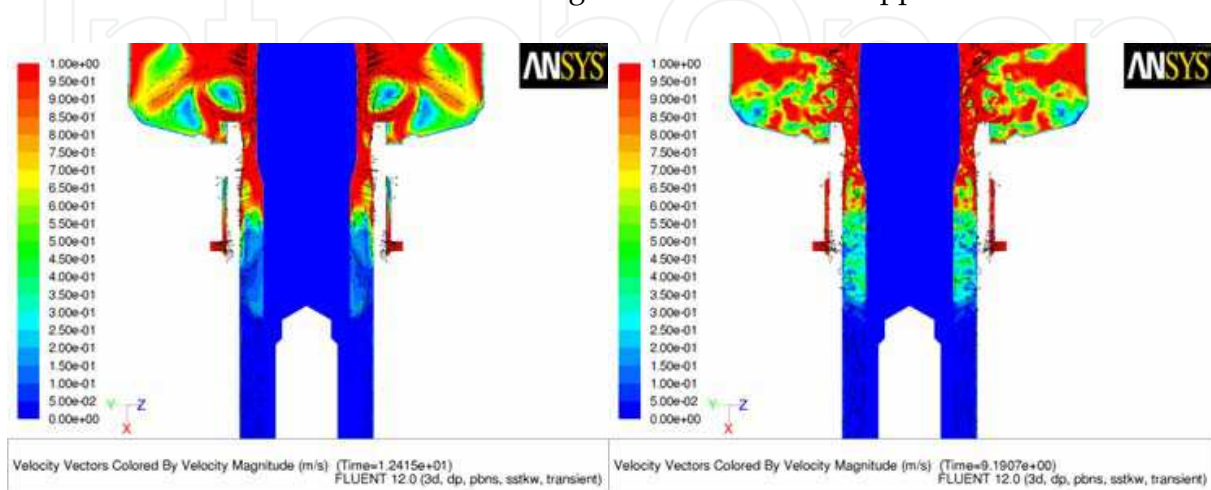


Fig. 5. Comparison of temperature and velocity fields, URANS to the left and VLES to the right ( $RCP = 0.38$ ), where finer structure may be observed.

The first case to be described here corresponds to the URANS simulation reported in Tinoco et al. (2010) concerning the mixing of cold and warm water within the annular space between a control rod and its corresponding guide tube. The URANS simulation is characterized by a high Reynolds number, strong disturbances and a high-resolution grid. Even if the numerical schemes of the FLUENT code are known to be rather dissipative, the simulated solution is strongly unsteady and exhibits rather large coherent structures caused by the inlet jets, as the example in the left view of Fig. 5 hints. Using the same grid and the same conditions, but smaller time steps, a simulation with the VLES approximation was tested with a value of  $RCP$  of 0.38, the same value as in Liu & Shih (2006), and the corresponding results are shown in the right view of Fig. 5. There, it is possible to observe structures of the URANS simulation accompanied with a rather wide range of smaller eddies indicating clearly that the simulated turbulence spectrum has been broadened. This test was discontinued due mainly to the increase in time involved in this type of simulation and to the lack of extensive validation of this rather novel approach. Also, the VLES approach gave a slightly poorer result in the test of CHT in a straight pipe, that will be reviewed in the next section (Tinoco et al., 2009).

The first real validation of the VLES approach carried out by the present authors consists of the simulation of the OECD/NEA-Vattenfall T-Junction Benchmark (OECD, 2010). Figure 6 below shows a comparison of the VLES simulation (right view), using  $RCP = 0.38$  and the same grid as in the URANS simulation shown in Fig. 4, with a DES simulation carried out in a coarser grid (left view). Both views in Fig. 6, which are instantaneous views of the

<sup>1</sup> During the process of editing the present chapter, it came to the knowledge of the authors that Nilsson & Gyllenram (2007) and Gyllenram & Nilsson (2008) have used an almost identical approach.

temperature field, differ radically from that of Fig. 4, showing that the unsteady solution is completely different in its behavior. Now, depending on the range of temperature differences and frequencies of the temperature fluctuations associated with the thermal striping phenomenon, the CHT to the wall may lead to high-cycle thermal fatigue (see e.g. Hosseini et al., 2009). Still, it is unclear if the unsteady CFD simulations may be able to accurately predict the thermal loading on the wall leading to thermal fatigue since no experiments on the heat flux to and out of a solid wall have yet been reported in the literature for validating this type of calculations. In the near future, experimental studies intended for CFD validation about the transient CHT between the flow inside the guide tube and the control rod will be carried out at Vattenfall Research and Development (VRD).

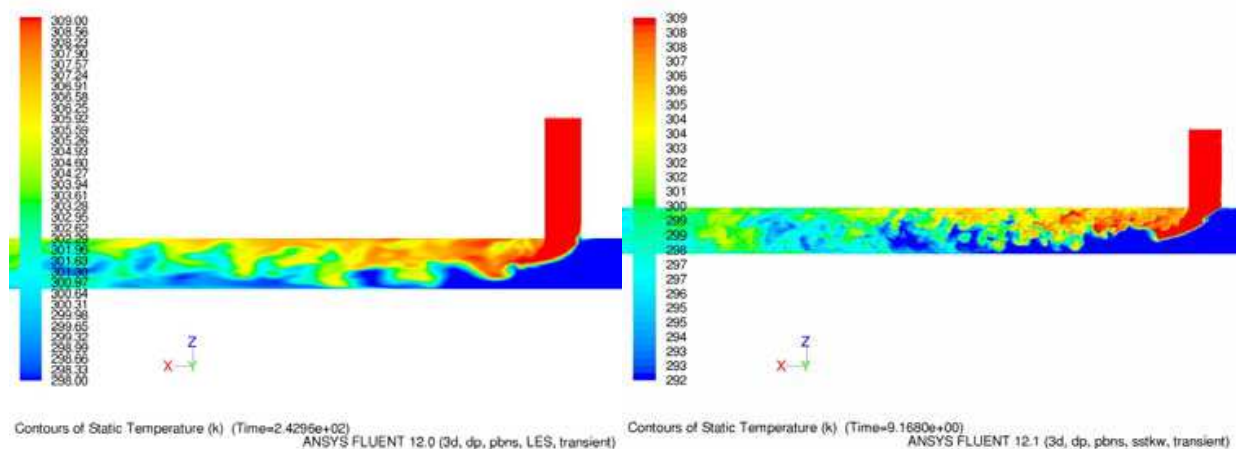


Fig. 6. Comparison of instantaneous temperature fields, DES to the left and VLES to the right ( $RCP = 0.38$ ), where finer structure may be observed due to finer grid.

### 3.3 Basic statistical validation examples

Even if the views in Fig. 6 give the impression of being physically correct, they constitute no quantitative proof of the accuracy of the simulation. In order to objectively validate the computational results against experimental values, a rather basic statistic comparison of not only the first order moments, the temporal mean values of the involved magnitudes, i.e. velocity and temperature, but also of the second order moments, the different variances or root-mean-square (rms) values, should be carried out. If  $\phi(x_i, t) = \{\phi_n(x_i, t_n), n = 1 \dots N\}$  is a turbulent stationary random variable given by its time series, then its temporal mean value is

$$\bar{\phi}(x_i) = \frac{1}{N} \sum_{n=1}^N \phi_n(x_i, t_n), \tag{11}$$

and its rms-value is

$$\phi_{rms}(x_i) = \sqrt{\frac{1}{N-1} \sum_{n=1}^N (\phi_n(x_i, t_n) - \bar{\phi}(x_i))^2}. \tag{12}$$

The sampling of the variable  $\phi(x_i, t) = \{\phi_n(x_i, t_n), n = 1 \dots N\}$  must fulfill some basic conditions like a broad population number (normally  $N \gg 10^3$ ) and a sampling rate (twice the Nyquist

frequency) which should be higher than twice the highest frequency contained in the fluctuations of  $\phi(x_i, t)$  (see e.g. Smith, 2007). Also, the sampling must take place when the simulation is statistically stationary, free from initial and other possible perturbations, i.e. the mean value of all variables associated with each point in the computational domain should have converged to a constant value.

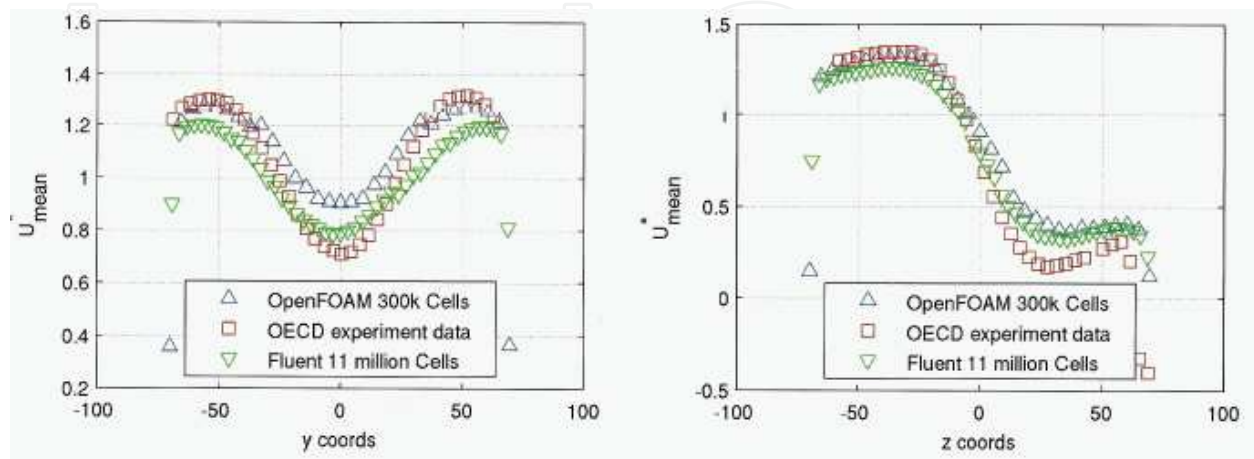


Fig. 7. Mean axial horizontal (left) and vertical (right) velocity profiles, 1.6-D downstream of the junction, for experiments (OECD, 2010), DES (OpenFoam) and VLES (FLUENT).

Figure 7 shows a comparison of the mean axial velocity profile, along a horizontal axis to the left and along a vertical axis to the right, at a section located 1.6 diameters (1.6-D) downstream of the tee-junction. The different values correspond to, respectively, experiments from the OECD/NEA-Vattenfall T-Junction Benchmark Exercise (OECD, 2010), DES with the open-source code OpenFoam (OpenCFD Ltd, 2004) and VLES with the FLUENT code. As may be observed from the results of this blind test, the agreement is fairly good for the temporal means of the axial velocity profile at this section, 1.6-D. For other sections and for the temporal mean of other components of the flow velocity, the agreement is similar but, for space reasons, these results have not been included in this work since they will be a part of the proceedings of the OECD/NRC & IAEA Workshop hosted by USNRC (OECD, 2010).

Figure 8 below shows the distribution of rms-value of axial velocity fluctuations along a horizontal axis to the left and along a vertical axis to the right, at a section located 1.6 diameters (1.6-D) downstream of the tee-junction. As in the preceding figure, the different values correspond to, respectively, experiments from the OECD/NEA-Vattenfall T-Junction Benchmark Exercise (OECD, 2010), DES with the open-source code OpenFoam and VLES with the FLUENT code.

As the results of Fig. 8 indicate, the agreement is fairly good even for the rms-values of the axial velocity fluctuations, as it is for other sections and for the second-order moments. Even if the preceding results are very encouraging regarding the performance of VLES, some general questions, to be discussed in what follows, are still not elucidated and need further investigation.

Figure 9 shows views of the mean axial velocity profile belonging to the same OECD case as in the preceding figures, and at the same section. In this figure, the blue curve corresponds to the experimental data and all other curves correspond to VLES simulations with different

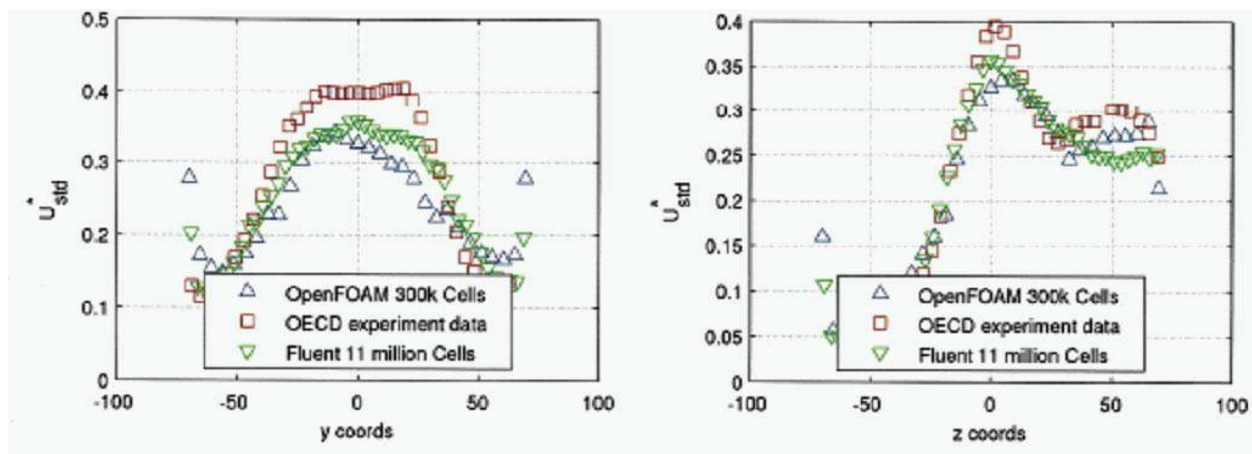


Fig. 8. Rms-value distribution of horizontal (left) and vertical (right) axial velocity fluctuations, 1.6-D downstream of the junction, for experiments (OECD, 2010), DES (OpenFoam) and VLES (FLUENT).

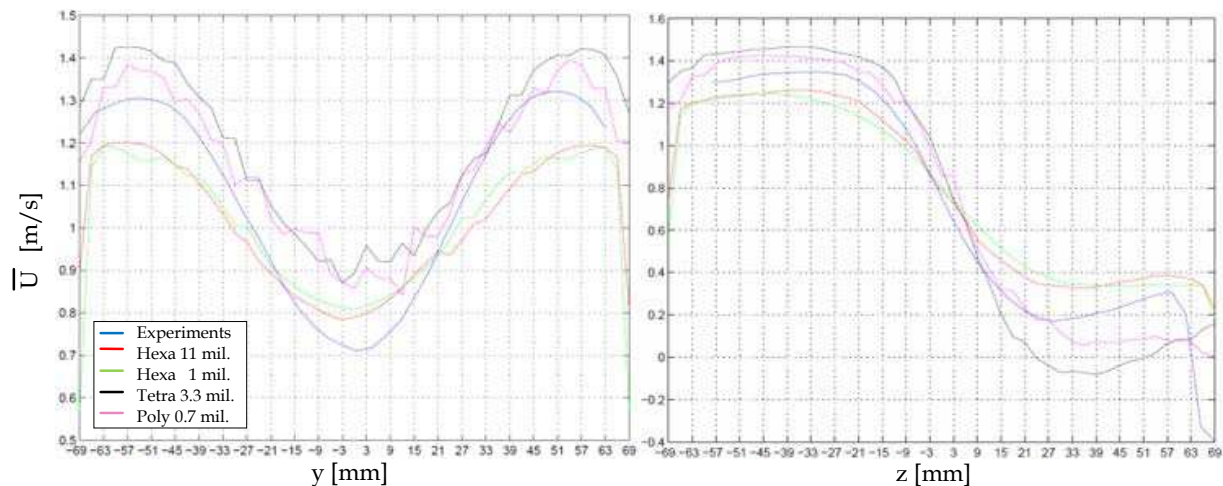


Fig. 9. Mean axial horizontal (left) and vertical (right) velocity profiles, 1.6-D downstream of the junction, for experiments (OECD, 2010) and four VLES (FLUENT) with different grids.

grids. The red curve corresponds to the abovementioned simulation with an 11 million hexahedral grid, the green curve to one with a 1 million hexahedral grid, the black curve to one with a 3.3 million tetrahedral grid and the pink curve to a simulation with a 0.7 million polyhedral grid.

Figure 10 shows rms-values of axial velocity fluctuations belonging to the same OECD case as in the preceding figures. As in Fig. 9, blue corresponds to the experiments, red to VLES with 11 million hexahedra, green to VLES with 1 million hexahedra, black to VLES with 3.3 million tetrahedra and pink to VLES with 0.7 million polyhedra. According to these two last figures, the general agreement between experiments and simulations is rather good for the mean velocity profile but, surprisingly enough, the best agreement is reached with the tetrahedral and polyhedral grids. This is also true for the rms-value of the axial velocity fluctuations except for the results obtained with the 1 million hexahedral grid that give rather poor agreement. Similar comparisons from other sections and/or other magnitudes, not included here for space reasons, corroborate the trend observed through the two

preceding figures. The unexpected outcome of this simulation exercise with different grids brings the problem associated with a clear definition of high-quality grid to the fore. Two preliminary conclusions may be drawn from the present discussion: firstly, that the quality of the grid seems to be associated with the simulated problem, and secondly, that polyhedral grids seem to keep what they promise about quality.

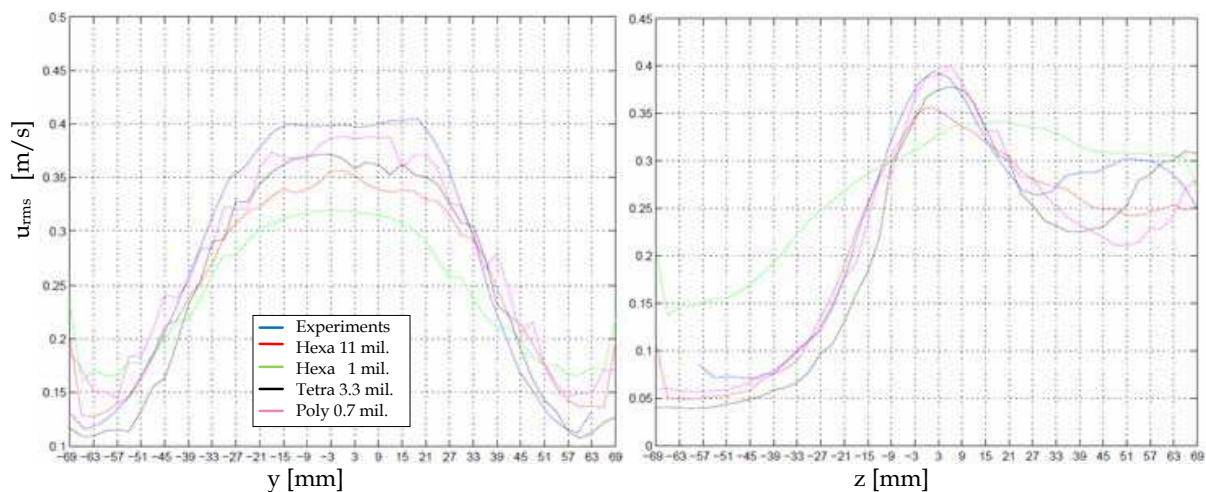


Fig. 10. Rms-value distribution of horizontal (left) and vertical (right) axial velocity fluctuations, 1.6-D downstream of the junction, for experiments (OECD, 2010) and four VLES (FLUENT) with different grids.

Finally, some other issues should be addressed in order to complete the view over numerical simulation of industrial flows using commercial codes. As the preceding paragraph suggests, the grid issue will probably need more time and effort to be resolved and, among other matters to be discussed, the definition of total simulation time needs perhaps a clarification. If the problem analyzed is statistically stationary, as it has been assumed until now, the convergence condition of the simulation is now twofold, first a solution convergence with each time step to minimize the numerical error and then a convergence of the solution to a statistically stationary solution. The later convergence implies a convergence of each point in the computational domain to a constant, time independent statistical mean. The corresponding boundary conditions of a statistically stationary simulation may contain time dependent constituents, like in the simulations of Davidson (2006) and Gilling et al. (2009) where synthetic turbulence is generated at the inlet, provided that the statistical temporal mean is constant.

Commercial codes are in general poorly adapted for running time dependant simulations since the sampling procedure is an operation not implemented at the same level as the case definition. User defined subroutines containing a number of suitable scripts are needed for generating text files of reduced size for sparing storage capacity since the normal data files produced by the code are too large. The capability for further statistical analysis of the sampled data in order to decide the degree of convergence of a time dependent simulation is practically non-existent in commercial CFD codes, and the user has to resort to other codes, like MATLAB (MathWorks, 2010), for the processing of the data.

Due to the amount of data that need to be processed, the selection and handling of images for the analysis of the time dependent simulation are crucial for understanding the problem studied and even for defining the simulation itself. As was mentioned before, the process of

defining the appropriate views in connection with the selection of a suitable combination of variables to be displayed is an iterative procedure that should be facilitated within the CFD code. In general, these options are, in the best case, insufficiently developed in the available commercial CFD codes and, as for the statistical data analysis, the user has to rely on additional software that may not be well adapted for the specific task. Probably, the visualization needs in industrial flow simulations may not be as advanced as those in scientific simulations of astrophysical phenomena (see e.g. Tohline, 2007) but a commercial CFD code containing tools similar to those used in science would undoubtedly win the appreciation of many industrial users. A complementary condition associated with visualization is that of a suitable format with satisfactory resolution quality, of the individual views and of the generated animated sequence that should produce the best possible result with minimized storage requirements.

#### 4. Heat transfer

Heat transfer, and more specifically CHT, deserves a special, although not necessary long, section for discussing its influence in industrial flow simulations since, depending on the case studied, it may constitute the cause of the problem. Indeed, together with cavitation and erosion-corrosion, thermal fatigue, both low cycle and high cycle, comprises one of the important mechanisms for damage generation of industrial equipment (see e.g. Zhu & Miller, 1998).

CFD simulation of heat transfer processes has progressively become an accepted tool for design, optimization, modification and safety analysis of industrial equipment. The applications of CHT reported in the literature range from cases of basic character such as the simulation of impinging cooling jets (Uddin, 2008, Zu et al., 2009) or nozzle flows (Marineau et al., 2006) to more applied cases like heat exchangers (Sridhara et al. 2005, Jayakumar et al., 2008), and to more advanced problems in nuclear reactors (Palko & Anglart, 2008, Tinoco & Lindqvist, 2009, Jo & Kang, 2010, Péniguel et al., 2010, Tinoco et al., 2010) and fusion reactors (Encheva et al., 2007).

Most of the examples mentioned above employ a URANS approach, implying that the Reynolds analogy between momentum transport and transport of heat through a turbulent Prandtl number is adopted in the simulations. Through this analogy, the turbulent transport of heat becomes locally isotropic and, normally, the turbulent Prandtl number is set to a constant value. However, even in flows of rather simple geometrical shape like a free impinging jet, the flow structure is complex, with clear anisotropic behavior near the wall, and with a turbulent Prandtl number which varies non-linearly over a rather definite range (Uddin, 2008). In this case, which is ill-suited for a URANS simulation, even a proper LES with the Smagorinsky-Lilly sub-grid model gives a Nusselt number distribution that fails to reproduce the location and intensity of the first maximum of the two-peaked experimental distribution (Uddin, 2008). In this work, the distance to the wall from cells adjacent to it is of the order of  $y^+ \approx 2 - 3$ , the streamwise dimension of the cells is  $r^+ \approx 36$  and the spanwise dimension  $r\Delta\theta^+ \approx 20$ . According to Tinoco et al. (2009) for pipe flow, and Veber & Carlsson (2010) for channel flow, the distance to the wall should be  $y^+ \leq 1$ , in order to be able to get the correct CHT. For channel flow, the streamwise dimensions should be  $x^+ \leq \sim 20$  and the spanwise dimensions  $z^+ \leq \sim 10$  (Veber & Carlsson, 2010). Probably similar requirements are to be fulfilled for the impinging jet flow but no study about the influence of the grid dimensions on CHT was carried out by Uddin (2008).

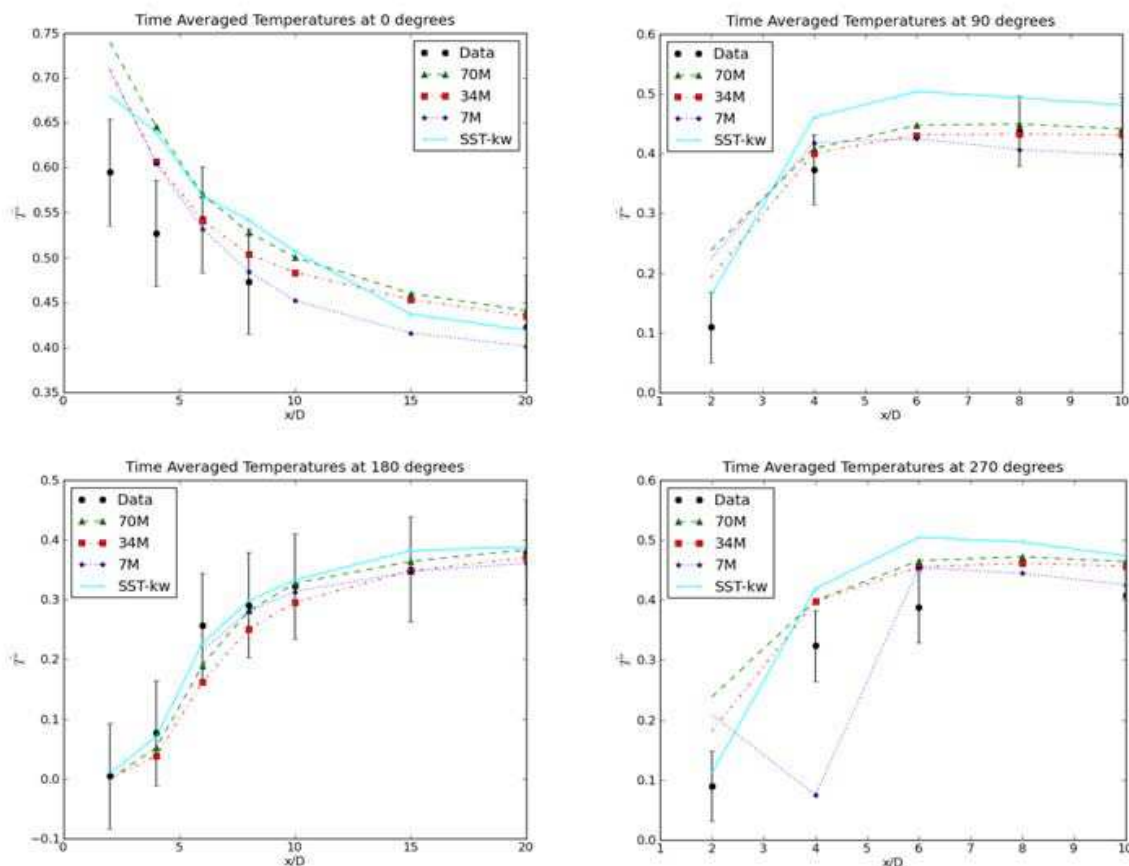


Fig. 11. Normalized axial mean temperature distribution at 1 mm from the wall for 4 azimuthal positions predicted using Fluent; LES with 3 grids (70 M, 34 M), VLES (SST-kw, 11 M) and experiments (OECD, 2010).

Curiously, a URANS simulation in steady mode of an impinging jet confined in a narrow gap using the SST model of turbulence gives satisfactory agreement with the experimental measurements of the Nusselt number distribution (Zu & Yan, 2009). In all probability, the walls of the cavity damp possible coherent structures that the jet might generate and the resulting Nusselt number distribution is flat, allowing even a URANS simulation to predict the distribution with an error of about 7%. Even if a study of grid sensitivity was performed in connection with the URANS simulation, the grid resolution is not expressed in wall friction units, making very difficult to decide if the resolution corresponds to the aforementioned requirements that are even valid for steady simulations (Palko & Anglart, 2008).

The case reported in Tinoco & Lindqvist (2009) and Tinoco et al. (2010) corresponds to a URANS simulation of unsteady CHT that tries to follow at least the grid requirement related to the normal distance to the wall. Due to the wide range of Reynolds numbers of the flow, the condition is only partially fulfilled even in the region most exposed to thermal loads. In any event, the results of the simulation compare well with the experimental measurements (Angele et al., 2010) of the temperature distributions in the fluid but the predictions of the CHT have not yet been compared with experiments. The measurements of heat flux in and out of the solid are far from trivial since the risk for perturbing the magnitude to be measured by the measuring device is very high. However, as was mentioned before,

measurements of the unsteady CHT will be carried out in the near future at VRD using multiple temperature measurements in the solid. With this experimental basis, simulations using URANS, VLES and DES/LES will be validated since other experimental foundations of unsteady CHT are essentially non-existent.

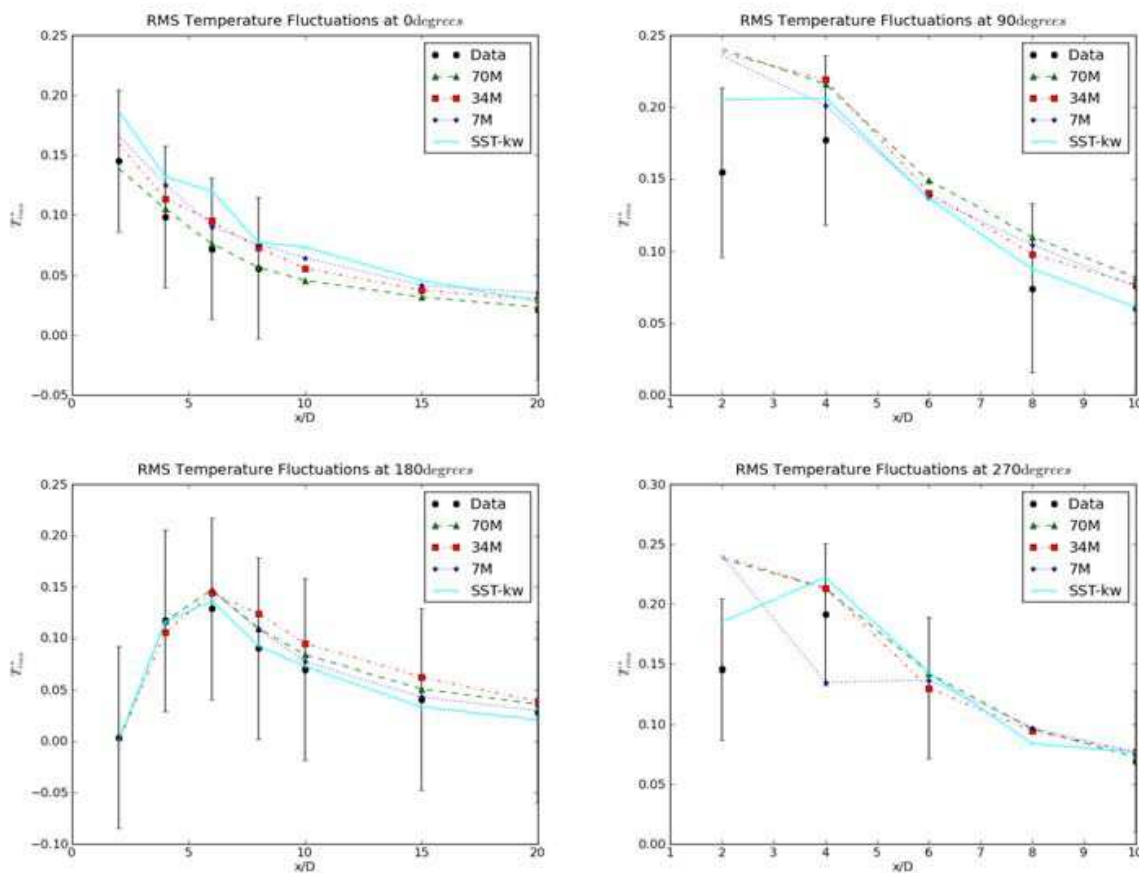


Fig. 12. Normalized axial distribution of rms-value of temperature fluctuations at 1 mm from the wall for 4 azimuthal positions predicted using Fluent; LES with 3 grids (70 M, 34 M), VLES (SST-kw, 11 M) and experiments (OECD, 2010).

Finally, some comments may be added about the simulation of turbulent heat transport within a fluid, excluding CTH. According to Fig. 4, the URANS approach to thermal mixing in a tee-junction lacks realism, at least for the grid, the numerical algorithm and the Reynolds number involved in the simulation. The corresponding VLES approach seems to capture the turbulent velocity field rather well, according to Figs. 8 and 9, indicating that the thermal mixing may be satisfactorily predicted. Surprisingly enough, the agreement between the predictions of the VLES approach with the 11 million grid together with a LES with three different grids and the experimental data (OECD, 2010) is not too good for the normalized (by temperature span) axial mean temperature distribution at the azimuthal positions of 0, 90 and 270 degrees for points located 1 mm from the wall, as Fig. 11 shows. This difference may be due to heat transfer effects since the pipes lack isolation. Heat transfer may affect to greater extent the upper part of the pipe that contains the warmer water with respect to the ambient temperature. A supporting indication is the fact that the temperature distribution at the azimuthal position of 180 degrees, i.e. the bottom of the pipe,

is very well predicted by simulations. This general trend is confirmed by the results of other simulations (see Mahaffy, 2010).

An additional indication of a systematic bias on the mean temperature measurements is constituted by the results shown in Fig. 12, where the normalized axial distribution of rms-value of temperature fluctuations is depicted. These rms-values are rather well predicted by the simulations, especially at the bottom of the pipe, i.e. at the azimuthal location of 180 degrees. The fact that temperature fluctuations mainly depend on the turbulence level, being less sensitive to heat transfer effects, may explain the aforementioned agreement displayed in Fig. 12. To sum up, and according to the results presented here about heat transfer and CHT, the VLES approach seems promising but the verifying simulations carried out in Tinoco et al. (2009) for steady CHT in a pipe indicate that the grid requirements for VLES of unsteady CHT may be similar, but not as severe, as those for a proper LES.

## 5. Verification and validation

The assessment of accuracy and reliability of numerical simulations, being not unique to the CFD methodology, is a necessary step in the process of solving a particular engineering or scientific problem. However, it might be of some interest to point out that accurate quantification of margins and uncertainties in CFD calculations is in particular important for two reasons. The first is due to the fact that CFD is often used as a replacement or complement to experimental investigation (in scaled or prototypic tests) of design or safety related problems. The other is that CFD is in many cases used to study three-dimensional fluid flow and heat transfer phenomena where there is a lack of previous experience (CFD application is outside the range of standard models and methods), for instance concerning mixing and stratification processes or heat transfer processes which require detailed investigation of phenomena in the fluid close to the solid wall (resolving boundary layers and turbulence modeling). Assessment of accuracy and reliability is in particular important when CFD is used in design and safety analyses of systems and processes which potentially can pose significant risk to the public and to the environment, such as nuclear power plants and some chemical industries. Actually, CFD applications in the field of nuclear reactor technology, both in the context of optimizing design and operation of power plants, as well as to solving safety issues, are rapidly growing in number. It is also a fact that rigorous requirements on accuracy assessment constitute today a limiting factor in the applicability of CFD for use in reactor safety cases.

Often the development of appropriate procedures and methodology for the assessment of accuracy and reliability of CFD simulations is driven by regulatory requirements. This is the case in the field of nuclear safety where high confidence in CFD simulations constitutes an obvious and necessary requirement. For example, in Sweden the regulatory authority, Swedish Radiation Safety Authority (SSM), requires that models, methods and data used to determine design and operating limits shall be validated and uncertainties shall be evaluated and analyzed. This applies to all kinds of deterministic analyses but, in the beginning, the requirement was intended for classical thermo-hydraulic codes used in the analysis of transients and accidents in nuclear power plants.

The process of assessment of credibility of CFD predictions usually contains two components, namely verification and validation. There are many definitions of these terms, which in some sense are variations around the same concept, with emphasis on certain

aspects of the verification and validation processes. In our opinion the following definitions are adequate (Oberkampf & Trucano, 2002):

- Verification: substantiation that a computerized model, i.e. computer code, represents a conceptual model within specified limits of accuracy.
- Validation: substantiation that a computerized model within its domain of applicability possesses a satisfactory range of accuracy consistent with the intended application of the model.

Popular, short descriptions of verification and validation also exist, namely that verification corresponds to “solving the equations right” and validation to “solving the right equations”. Interested readers are referred to the work of Roache (1997), Oberkampf & Trucano (2002), Roy (2005) and Stern et al. (2006) or the guidelines published by AIAA (1998), ERCOFTAC (2000), NEA (2007) and ASME (2009) for more information concerning verification and validation in CFD.

In the opinion of Oberkampf and Trucano (2002), the above definition of validation can be considered as somewhat vague. This definition, however, captures an essential aspect of CFD applications, namely that the requirement on the level of accuracy must be adapted to the parameters involved in the particular application and to the purpose of the simulations. For instance, in applications to problems in assessment of safety of nuclear power plants, the requirement on validation and accuracy must be, in general, high. However, even in this application field the requirement on validation is often a compromise based on the overall assessment of the problem, in which considerations including the purpose of the CFD analysis, simulations with less detailed codes and limited experimental validation must be weighted together to guide in the decision process. In some cases even qualitative insights into a particular problem provided by CFD results can be very useful. Hence, validation cannot be disconnected from a particular problem at hand but should be performed and evaluated in the context of what is reasonable and acceptable in each particular case. For instance, when CFD is used to provide input to structural mechanics codes for analysis of structural response to thermal loads (e.g. thermal fatigue), it is reasonable to adjust the requirement on the accuracy of CFD simulations to the desired accuracy in the input to structural analysis code.

Verification is achieved through comparison to exact analytical solutions, manufactured solutions or previously verified higher order simulations. The goal of verification is quantification of errors associated with insufficient spatial discretization convergence, insufficient temporal discretization convergence, lack of iterative convergence, and computer programming as well as with specification of initial and boundary conditions in an input model. According to the available standards and guidelines (AIAA 1998, NEA, 2007, ASME, 2009), verification testing relies on a systematic refinement of the grid size and time step to estimate the discretization error of the numerical solution. However, this procedure might give a wrong answer in the case of DES, as was commented before. In general, both the ASME standard and the aforementioned Guides assume steady solutions or time-averaged solutions, giving therefore no uncertainty estimation procedure for unsteady solutions containing statistical magnitudes for describing the simulation results. The new direction of industrial CFD towards full time-dependent simulations does not seem to have been noticed or forecasted by the different groups involved in developing guidelines and standards for verification and validation. Therefore, the comparison report

of the OECD/NEA-Vattenfall T-junction Bench mark Exercise (Mahaffy, 2010) is a very good example of the difficulties associated with the quality assessment of this type of simulations and, at the same time, it might constitute a first base in the development of criteria for error estimation, verification and validation.

Validation is achieved through the comparison between computational results and experimental data. Assessment of experimental uncertainties is a very important element of validation process. Considering that real engineering systems are often complex in terms of complicated geometry and many coupled physical phenomena, Oberkampf and Trucano (2002) have recommended a tiered approach to validation. The studied system is divided into four progressively simpler tiers that may lead to a minimization of the cancellation error problem.

- Complete systems
- Subsystems cases
- Benchmark cases
- Unit problems

In this approach, the validation starts from the unit problem, where only one phenomenon is investigated, often in simplified geometry but in well instrumented facility. The advantage of the tiered approach is that the four tiers together provide satisfactory validation even if complete validation on the subsystems or complete systems is practically impossible due to the lack of necessary measurements.

In the case of complex engineering systems, the selection of experiments used for validation might be guided by the PIRT process (Phenomena Identification and Ranking Table), a process originated as part of the U.S. Nuclear Regulatory Commission Code Scaling, Applicability and Uncertainty evaluation methodology (see e. g. NEA, 2007). In PIRT, phenomena and processes are ranked based on their influence on appropriate criteria, e.g. nuclear reactor safety criteria. Target variables should be selected by a panel of experts.

Statistical uncertainty analysis, using a Monte Carlo approach, which is often performed in numerical simulations, is in the case of CFD simulations of more complex systems practically impossible due to limitations in time and computer resources.

It is essential that the process and results of verification and validation are properly documented. Code verification should primarily be the responsibility of the code supplier (code developer), particularly if it concerns a commercial code, and should follow some general standard such the ASME standard V&V 20-2009 (ASME, 2009). As NEA's Guide suggests, every supplier of a commercial code should provide all users and even interested regulatory authorities, with a complete documentation of the verification. This demand seems legitimate because users have very seldom access to the source code of a commercial program that has to be used as a black box. At the same time, and owing to fact the user produces a solution, the verification of which is his responsibility, the user shares the responsibility of the verification of the code that generated the solution. Therefore, the user has the obligation of reporting the deficiencies detected through the use of the code, which should be of public knowledge to warn other users and to force the code supplier to deal with them. The burden of validation, which is a process that may involve expensive experimental activities, has to be shared by the complete CFD community, but principally by the industry that most directly harvests the fruits of well validated CFD simulations.

## 6. Acknowledgement

The authors want to thank Nicolas Forsberg from Forsmarks Kraftgrupp AB for allowing the use of his OpenFoam results in this paper.

## 7. References

- Acikgoz, N., (2007). Adaptive and Dynamic Meshing Methods for Numerical Simulations, Doctoral Thesis, Georgia Institute of Technology, Atlanta, GA, USA.
- AIAA, (1998), Guide for the Verification and Validation of Computational Fluid Dynamics Simulations, AIAA Guide G-077-1988, ISBN 1-56347-285-6, January 14, 1998.
- ASME, (2009). Standard for Verification and Validation in Computational Fluid Dynamics and Heat Transfer, *The American Society of Mechanical Engineers*, ASME V&V 20-2009.
- Angele, K., Cehlin, M., Högström, C-M., Odemark, Y., Henriksson, M., H., Lindqvist, H. & Hemström, B. (2010). Flow Mixing Inside a Control-Rod Guide Tube – Part II: Experimental Tests and CFD-Validation, *18<sup>th</sup> International Conference on Nuclear Engineering (ICONE 18)*, Xi'an, China.
- ANSYS Fluent (2006). "Fluent 6.3 Documentation", Fluent Inc., Lebanon, NH (2006).
- Beall, M. W., Walsh, J. & Shephard, M. S. (2003). Accessing CAD Geometry for Mesh Generation, *12<sup>th</sup> International Meshing Roundtable*, Sandia National Laboratories, New Mexico, USA.
- Borouchaki, H. & Frey, P. J. (1998). Adaptive Triangular-Quadrilateral Mesh Generation, *Int. J. Numer. Meth. Engng.*, Vol. 41, pp. 915-934.
- Davidson, L., (2006). Evaluation of the SST-SAS Model: Channel Flow, Asymmetric Diffuser and Axi-Symmetric Hill, *European Conference on Computational Fluid Dynamics, ECCOMAS CFD 2006*, TU Delft, The Netherlands.
- de Hauteclocque, G., Dix, J., Lamkin, D. & Turnock, S. (2007). Flow and Likely Scour Around Three Dimensional Seabed Structures Evaluated Using RANS CFD, University of Southampton, Ship Science Report No. 144, September 2007.
- Dietiker, J. F. & Hoffmann, K. A., (2009). Predicting Wall Pressure Fluctuations Over a Backward-Facing Step Using Detached Eddy Simulation, *J. of Aircraft*, Vol. 46, No. 6, pp. 2115-2120.
- Doering, C. R. (2009). The 3D Navier-Stokes Problem, *Annu. Rev. Fluid Mech.*, Vol. 42, pp. 109-128.
- Duraisamy, K. & Iaccarino, G., (2005). Curvature Correction and Application of the  $v^2-f$  Turbulence Model to Tip Vortex Flows, *Center for Turbulence Research, Annual Research Briefs 2005*, Stanford University, Stanford, California, USA.
- Encheva, A., Vayakis, G., Chavan, R., Karpouchov, A. & Moret, J. M., (2007). 3D Thermal and CFD Simulations of the Divertor Magnetic Coils for ITER, *NAFEMS World Congress 2007 (Simul. Technol. for the Eng. Analysis Community)*, Vancouver, Canada, 22 May 2007.
- ERCOFTAC, (2000). Best Practice Guidelines, *European Research Community On Flow, Turbulence And Combustion (ERCOFTAC), Special Interest Group on "Quality and Trust in Industrial CFD"*, Version 1.0 January 2000.

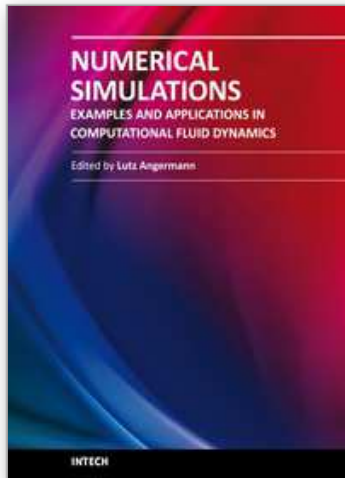
- Fadai-Ghotbi, A., Friess, C., Manceau, R., Gatski, T. B. & Borée, J., (2010). Temporal Filtering: A Consistent Formalism for Seamless Hybrid RANS-LES Modeling in Inhomogeneous Turbulence.
- Fluent, (2006). GAMBIT 2.3 User's Guide, Fluent Incorporated, Lebanon, NH, USA.
- Forsythe, J. R., Hoffmann, K. A., Cummings, R. M. & Squires, K. D., (2002). Detached-Eddy Simulation With Compressibility Corrections Applied to a Supersonic Axisymmetric Base Flow, *J. Fluids Engng.*, Vol. 124, pp. 911-923.
- Gilling, L., Sørensen, N. N. & Davidson, L., (2009). Detached Eddy Simulation of an Airfoil in Turbulent Inflow, *47<sup>th</sup> AIAA Aerospace Sciences Meeting Including The New Horizons Forum and Aerospace Exposition, AIAA Paper 2009-270*, 5-8 January 2009, Orlando, Florida, USA.
- Gyllenram, W. & Nilsson, H., (2008). Design and Validation of a Scale-Adaptive Filtering Technique for LRN Turbulence Modeling of Unsteady Flow, *J. Fluids Engng.*, Vol. 130, pp. 051401-1 - 051401-10.
- Hamba, F., (2009). Log-Layer Mismatch and Commutation Error in Hybrid RANS/LES Simulation of Channel Flow, *Int. J. Heat Fluid Flow*, Vol. 30, pp. 20-31.
- Hamed, A., Basu, D. & Das, K. (2003). Detached Eddy Simulation of Supersonic Flow Over a Cavity, *AIAA Paper 2003-0549, 41<sup>st</sup> AIAA Conference*, Reno, Nevada, USA.
- Hartmann, H., Derksen, J. J., Montavon, C., Pearson, J., Hamill, I. S. & van den Akker, H. E. A. (2004). Assessment of Large Eddy and RANS Stirred Tank Simulations by Means of LDA, *Chem. Engng. Sci.*, Vol. 59, pp. 2419-2432.
- Hosseini, S. M., Yuki, K. & Hashizume, H., (2009). Experimental Investigation of Flow Field Structure in Mixing Tee, *J. Fluids Engng.*, Vol. 131, pp. 051103-1 - 051103-7.
- Hsieh K. J., Lien, F. S. & Yee, E. (2010). Towards a Unified Turbulence Simulation Approach for Wall-Bounded Flows, *Flow Turb. Combust.*, Vol. 84, pp. 193-218.
- Höhne, T., Krepper, E. & Rohde, U., (2010). Application of CFD Codes in Nuclear Reactor Safety Analysis, *Sci. Tech. Nuclear Inst.*, Vol. 2010, Article ID 198758, 8 pp.
- Ishihara, T., Gotoh, T. & Kaneda, Y. (2009). Study of High-Reynolds Number Isotropic Turbulence by Direct Numerical Simulation, *Annu. Rev. Fluid Mech.*, Vol. 41, pp. 165-180.
- Jayakumar, J. S. Mahajani, S. M., Mandal, J. C., Vijayan, P. K. & Bhoi, R., (2008). Experimental and CFD Estimation of Heat Transfer in Helically Coiled Heat Exchangers, *Chem. Eng. Research Design*, Vol. 86, No. 3, pp. 221-232.
- Jo, J. C. & Kang, D. G., (2010). CFD Analysis of Thermally Stratified Flow and Conjugate Heat Transfer in a PWR Pressurizer Surge Line, *J. Press. Vessel Tech.*, Vol. 132, pp. 021301-1 - 021301-10.
- Jones, W. P. & Launder, B. E., (1973), The Calculation of Low-Reynolds-Number-Phenomena with a Two-Equation Model of Turbulence, *Int. J. Heat Mass Transf.*, Vol. 16, pp. 1119-1130.
- Kim, S. E., Rhee, S. H. & Cokljat, D., (2005). The Prolate Spheroid Separates Turbulence Models, *Fluent News*, Spring 2005, pp.12-13.
- King, A. J. C. & Jagannatha, D., (2009). Simulation of Synthetic Jets With Non-Sinusoidal Forcing Functions for Heat Transfer Applications, *18<sup>th</sup> World IMACS/MODSIM Congress*, Cairns, Australia, 13-17 July, 2009, pp. 1732-1738.
- Kline, S. J., (1989). Zonal Modeling, Stanford University, Thermosciences Division, Final Report, 1 Jan. 1986 - 31 Dec. 1988.

- Kolmogorov, A. N. (1941). The Local Structure of Turbulence in Incompressible Viscous Fluid for Very Large Reynolds Number, *Dokl. Akad. Nauk. SSSR*, Vol. 30(4), pp. 301-305.
- Lal, A. & Elangovan, M., (2008). CFD Simulation and Validation of Flap Type Wave-Maker, *World Academy of Sciences, Engng. Tech.*, Vol. 46, pp. 76-82.
- Li, Z., (2007). Numerical Simulation of Sidewall Effects on Acoustic Fields in Transonic Cavity Flow, University of Cincinnati, Department of Aerospace Engineering and Engineering Mechanics of the College of Engineering, Master of Science Thesis, March 2007.
- Liu, N. S. & Shih, T. H., (2006). Turbulence Modeling for Very Large-Eddy Simulation, *AIAA Journal*, Vol. 44, pp. 687-697.
- Lynch, G. E. & Smith, M. J., (2008). Hybrid RANS-LES Turbulence Models on Unstructured Grids, *38<sup>th</sup> Fluid Dynamic Conference and Exhibit, AIAA Paper 2008-3854*, 23-26 June 2008, Seattle, Washington, USA.
- Mahaffy, J., (2010). Synthesis of Results for the Tee-Junction Benchmark, *CFD4NRS-3, Experimental Validation and Application of Computational Fluid Dynamics and Computational Multi-Fluid Dynamics Codes to Nuclear Reactor Safety Issues*, OECD/NRC & IAEA Workshop hosted by USNRC, September 14-16 2010, Washington D.C., USA.
- Marineau E. C., Schetz, J. A. & Neel, R. E., (2006). Turbulent Navier-Stokes Simulations of Heat Transfer with Complex Wall Temperature Variations, *9<sup>th</sup> AIAA/ASME Joint Thermophysics and Heat Transfer Conference, AIAA Paper AIAA-2006-3087*, June 5-8, 2006, San Francisco, California.
- MathWorks, (2010). MATLAB Technical Documentation, <http://www.mathworks.se/>.
- Menter, F. R. (1994). Two-Equation Eddy-Viscosity Turbulence Models for Engineering Applications, *AIAA Journal*, Vol. 32, No. 8, pp. 1598-1605.
- Menter, F. R. (2009). Review of the Shear-Stress Transport Turbulence Model Experience From an Industrial Perspective, *Int. J. Com. Fluid Mech.*, Vol. 23, No. 4, pp. 305-316.
- Menter, F. R., Kuntz, M. & Langtry, R. (2003). Ten Years of Industrial Experience with the SST Turbulence Model, *4<sup>th</sup> International Symposium on Turbulence, Heat and Mass Transfer, ICHMT 4*, Antalya, Turkey.
- Menter, F. R., Kuntz, M. & Bender, R., (2003). A Scale-Adaptive Simulation Model for Turbulent Flow Prediction, *AIAA Paper 2003-0767*, Reno, Nevada, USA.
- Menter, F. R. & Egorov, Y., (2004). Revisiting the Turbulent Length Scale Equation, *IUTAM Symposium: One Hundred Years of Boundary Layer Research*, Göttingen, Germany.
- Menter, F. R. & Egorov, Y., (2005). A Scale-Adaptive Simulation Model Using Two-Equation Models, *AIAA Paper 2005-1095*, Reno, Nevada, USA.
- Morton S. A., Cummings, R. M. & Kholodar, D. B., (2004). High Resolution Turbulence Treatment Of F/A-18 Tail Buffet, *45<sup>th</sup> AIAA/ASME,ASCE/AHS/ASC Structures, Structural Dynamics & Materials Conference, AIAA Paper 2004-1676*, 19-22 April, 2004, Palm Springs, California, USA.
- Nilsson, H. & Gyllenram, W., (2007). Experiences with Open FOAM for water turbines applications, *Proceedings of the 1st OpenFOAM International Conference, 26-27 November 2007*, Beaumont House, Old Windsor, United Kingdom.

- NEA, (2007). Best Practice Guidelines for the Use of CFD in Nuclear Reactor Safety Applications, *Nuclear Energy Agency, Committee on the Safety of Nuclear Installations*, NEA/CSNI/R(2007)5, May 15, 2007.
- Oberkampf, W., L. & Trucano, T., G. (2002). Verification and Validation in Computational Fluid Dynamics, *Progress in Aerospace Sciences*, 38: 209-272.
- OECD, (2010). OECD/NEA-Vattenfall T-Junction Benchmark Exercise: Thermal Fatigue in a T-junction, *CFD4NRS-3, Experimental Validation and Application of Computational Fluid Dynamics and Computational Multi-Fluid Dynamics Codes to Nuclear Reactor Safety Issues*, OECD/NRC & IAEA Workshop hosted by USNRC, September 14-16 2010, Washington D.C., USA.
- OpenCFD Ltd, (2004). OpenFOAM open source CFD toolbox, <http://www.openfoam.com>.
- Orszag, S. A. (1970). Analytical Theories of Turbulence, *J. Fluid Mech.*, Vol. 41, pp. 363-386.
- Palko, D. & Anglart, H., (2008). Theoretical and Numerical Study of Heat Transfer Deterioration in High Performance Light Water Reactor", *Sci. Tech. Nucl. Instal.*, ID 405072.
- Péniguel, C., Rupp, I., Rolfo, S. & Guillaud, M., (2010). Thermal-Hydraulics and Conjugate Heat Transfer Calculation in a Wire-Wrapped SFR Assembly, *International Congress on Advances in Nuclear Power Plants, ICAPP '10*, June 13-17, 2010, San Diego, California, USA.
- Peric, M (2004). Flow Simulation Using Control Volumes of Arbitrary Polyhedral Shape, *ERCOFTAC Bulletin No. 62*, September, 2004, pp. 25-29.
- Perot, J. B. & Gadebusch, J., (2007). A Self-Adapting Turbulence Model for Flow Simulation at Any Mesh Resolution, *Phys. Fluids*, Vol. 19, pp. 115105-1 - 115105-11.
- Perot, J. B. & Gadebusch, J., (2009). A Stress Transport Equation Model for Simulating Turbulence at Any Mesh Resolution, *Teor. Comput. Fluid Dyn.*, Vol. 23, pp. 271-286.
- Pope, S. B. (2000). *Turbulent Flows*, Cambridge University Press, ISBN 0-521-59886-9, UK.
- Roache, P., J., (1997). Quantification of Uncertainty in Computational Fluid Dynamics, *Annu. Rev. Fluid. Mech.* 29: 123-160.
- Roy, C., J. (2005). Review of Code and Solution Verification Procedures for Computational Simulation, *Journal of Computational Physics*, 205, 131-156.
- Rumsey, C. L., (2004). Computation of a Synthetic Jet in a Turbulent Cross-Flow Boundary Layer, *NASA Report, TM-2004-213273*.
- Ruprecht, A., Helmrich, T. & Buntic, I. (2003). Very Large Eddy Simulation for the Prediction of Unsteady Vortex Motion, *Conference on Modelling Fluid Flow (CMFF'03)*, The 12<sup>th</sup> International Conference on Fluid Flow Technologies, Budapest, Hungary, September 3-6, 2003.
- Shih, T. H. & Liu, N. S. (2006). A Strategy for Very Large Eddy Simulation of Complex Turbulent Flows, *44<sup>th</sup> AIAA Aerospace Sciences Meeting and Exhibit, AIAA Paper 2006-175*, January 9-12, 2006, Reno, Nevada, USA.
- Shih, T. H. & Liu, N. S. (2008). Assessment of the Partially Resolved Numerical Simulation (PRNS) Approach in the National Combustion Code (NCC) for Turbulent Non-Reacting and Reacting Flows, *NASA Report NASA/TM-2008-215418*, October 2008.
- Shih, T. H. & Liu, N. S., (2009). A Very Large Eddy Simulation of the Non-Reacting Flow in a Single-Element Lean Direct Injection Combustor Using PRNS with Nonlinear Subscale Model, *NASA Report NASA/TM-2009-215644*, August 2009.

- Shih, T. H. & Liu, N. S., (2010). A Nonlinear Dynamic Subscale Model for Partially Resolved Numerical Simulation (PRNS)/Very Large Eddy Simulation (VLES) of Internal Non-Reacting Flows, *NASA Report NASA/TM-2010-216323*, May 2010.
- Smirnov, P., Hansen, T. & Menter, F. R., (2007). Numerical Simulation of Turbulent Flows in Centrifugal Compressor Stages with Different Radial Gaps, *Proceedings of GT2007, ASME Turbo Expo 2007: Power for Land, Sea and Air*, May 14-17, Montreal, Canada.
- Smith, S. W., (2007). *The Scientist and Engineer's Guide to Digital Signal Processing*, California Technical Publishing, California, USA.
- Spalart, P. R., Jou, W. -H., Strelets, M. & Allmaras, S. R. (1997). Comments on the Feasibility of LES for Wings, and on a Hybrid RANS/LES approach, 1<sup>st</sup> AFOSR International Conference on DNS/LES, August 4-8, 1997, Ruston, Los Angeles, In *Advances in DNS/LES*, Liu & Z. Liu Eds., Greyden Press, Columbus, Ohio, 1997.
- Spalart, P. R. (2009). Detached-Eddy Simulations, *Annu. Rev. Fluid Mech.*, 41, pp.181-202.
- Sridhara, S. N., Shankapal, S. R. & Umesh Babu, V. (2005). CFD Analysis of Fluid Flow and Heat Transfer in a Single Tube-Fin Arrangement of an Automotive Radiator, *International Conference on Mechanical Engineering, ICME2005*, December 28-30, 2005, Dhaka, Bangladesh.
- Stern, F., Wilson, R. & Shao, J. (2006). Quantitative V&V of CFD simulations and certification of CFD codes, *International Journal for Numerical Methods in Fluids*, 50: 1335-1355.
- Tinoco, H. (2002). Three-Dimensional Modeling of a Steam-Line Break in a Boiling Water Reactor, *Nuc. Sci. Engng.*, Vol. 140, No. 2, pp. 152-164.
- Tinoco, H. & Hemström, B. (1990). Numerical Modeling of Two-Phase Flow in the Upper Plenum of a BWR by a Three-Dimensional Two-Fluid Model, *International Symposium on Engineering Turbulence Modeling and Measurements*, pp. 927-936, ISBN13: 9780444015631, ISBN10: 0444015639, Dubrovnik, Yugoslavia, September 24-28, Elsevier, New York.
- Tinoco, H. & Einarsson, T. (1997). Numerical Analysis of the Mixing and Recombination in the Downcomer of an Internal Pump BWR, *Eighth International Topical Meeting on Nuclear Reactor Thermal-Hydraulics (NURETH 8)*, Kyoto, Japan.
- Tinoco, H, Darelius, A., Bernerskog, E., & Lindqvist, H., (2009). Forsmark 3 – System 30-222. Control rods. Time Dependent Flow Simulations of the Mixing Process Between the Crud-Cleaning Flow and the Bypass Flow Inside the Control Rod Guide Tube, *FKA Report FT-2009-2732*, 2009-09-02, Forsmark, Sweden.
- Tinoco, H. & Lindqvist, H., 2009. Thermal Mixing Instability of the Flow Inside a Control-Rod Guide Tube, *Thirteenth International Topical Meeting on Nuclear Reactor Thermal-Hydraulics (NURETH 8)*, Kanazawa, Japan.
- Tinoco, H. & Ahlinder, S. (2009). Mixing Conditions in the Lower Plenum and Core Inlet of a Boiling Water Reactor, *J. Engng. Gas Turb. Power*, Vol. 131, Paper No. 062903, pp. 1-12.
- Tinoco, H., Lindqvist, H., Odemark, Y., Högström, C-M. & Angele, K., (2010). Flow Mixing Inside a Control-Rod Guide Tube – Part I: CFD Simulations, *18<sup>th</sup> International Conference on Nuclear Engineering (ICONE 18)*, Xi'an, China.
- Tohline, J. E., (2007). Scientific Visualization: A Necessary Chore, *Computing in Science and Eng.*, Vol. 9, No. 6, pp. 76-81.

- Uffinger, T., Becker, S. & Ali, I., (2010). Vortex Dynamics in the Wake of Wall-Mounted Cylinders: Experiments and Simulation, *15<sup>th</sup> International Symposium on Applications of Laser Techniques to Fluid Mechanics*, Lisbon, Portugal, 5-8 July, 2010.
- Uddin, N., (2008). Turbulence Modeling of Complex Flows in CFD, Doctoral Thesis, Institute of Aerospace Thermodynamics, University of Stuttgart, August 2008, Germany.
- Vatsa, V. N. & Turkel, E. L., (2004). Simulation of Synthetic Jets in Quiescent Air Using Unsteady Reynolds Averaged Navier-Stokes Equations, *22<sup>nd</sup> AIAA Applied Aerodynamics Conference and Exhibit*, August 16-19, Providence, Rhode Island, USA.
- Veber, P. (2009). O3 - LES Analysis of the Mixing Region Between Bypass Flow and Crud-Cleaning Flow, (in Swedish), *Onsala Ingenjörbyrå*, Technical Note 01, 2009, Gothenburg, Sweden.
- Veber, P. & Carlsson, F., (2010). Heat Transfer Validation in Turbulent Channel Flow using Large Eddy Simulations, *Inspecta, Nuclear Technology 2010, Nordic Symposium*, December 1-2 2010, Stockholm, Sweden.
- Wilcox, D. C., (1988). Reassessment of the Scale-Determining Equation for Advanced Turbulence Models, *AIAA Journal*, Vol. 26, pp. 1299-1310.
- Wilcox, D. C., (1994). *Turbulence Modeling for CFD*, DCW Industries, Inc., ISBN 0-9636051-0-0, La Cañada, California, USA.
- Woodard, P. R., Batina, J. T. & Yang, H. T. Y., (1992). Quality Assessment of Two- and Three-Dimensional Unstructured Meshes and Validation of an Upwind Euler Flow Solver, NASA Technical Memorandum 104215.
- Young, M. E. & Ooi, A., (2004). Turbulence Models and Boundary Conditions for Bluff Body Flow, *15<sup>th</sup> Australian Fluid Mechanics Conference, The University of Sydney, Sydney, Australia*, 13-17 December 2004.
- Zaki, M., Menon, S. & Sankar, L., (2010). Hybrid Reynolds-Averaged Navier-Stokes and Kinetic Eddy Simulation of External and Internal Flows, *J Aircraft*, Vol. 47, No. 3, pp. 805-811.
- Zhai, Z., Zhang, Z., Zhang, W. & Chen, Q., (2007). Evaluation of Various Turbulence Models in Predicting Airflow and Turbulence in Enclosed Environments by CFD: Part-1: Summary of Prevalent Turbulence Models, *HVAC&R Research*, Vol. 13, No. 6, pp. 853-870.
- Zhai, Z., Zhang, Z., Zhang, W. & Chen, Q., (2007). Evaluation of Various Turbulence Models in Predicting Airflow and Turbulence in Enclosed Environments by CFD: Part 2— Comparison with Experimental Data from Literature, *HVAC&R Research*, Vol. 13, No. 6, pp. 871-886.
- Zhu, D. & Miller, R. A., (1998). Investigation of Thermal High Cycle and Low Cycle Fatigue Mechanisms of Thick Thermal Barrier Coatings, *NASA Report NASA/TM-1998-206633*, February 1998.
- Zu, Y. Q., Yan, Y. Y. and Maltson, J. (2009). Numerical Study of Stagnation Point Heat Transfer by Jet Impingement in a Confined Narrow Gap, *J. Heat Transfer*, Vol. 131, pp. 094504-1 - 094504-4.



## **Numerical Simulations - Examples and Applications in Computational Fluid Dynamics**

Edited by Prof. Lutz Angermann

ISBN 978-953-307-153-4

Hard cover, 440 pages

**Publisher** InTech

**Published online** 30, November, 2010

**Published in print edition** November, 2010

This book will interest researchers, scientists, engineers and graduate students in many disciplines, who make use of mathematical modeling and computer simulation. Although it represents only a small sample of the research activity on numerical simulations, the book will certainly serve as a valuable tool for researchers interested in getting involved in this multidisciplinary field. It will be useful to encourage further experimental and theoretical researches in the above mentioned areas of numerical simulation.

### **How to reference**

In order to correctly reference this scholarly work, feel free to copy and paste the following:

Hernan Tinoco, Hans Lindqvist and Wiktor Frid (2010). Numerical Simulation of Industrial Flows, Numerical Simulations - Examples and Applications in Computational Fluid Dynamics, Prof. Lutz Angermann (Ed.), ISBN: 978-953-307-153-4, InTech, Available from: <http://www.intechopen.com/books/numerical-simulations-examples-and-applications-in-computational-fluid-dynamics/numerical-simulation-of-industrial-flows>

**INTECH**  
open science | open minds

### **InTech Europe**

University Campus STeP Ri  
Slavka Krautzeka 83/A  
51000 Rijeka, Croatia  
Phone: +385 (51) 770 447  
Fax: +385 (51) 686 166  
[www.intechopen.com](http://www.intechopen.com)

### **InTech China**

Unit 405, Office Block, Hotel Equatorial Shanghai  
No.65, Yan An Road (West), Shanghai, 200040, China  
中国上海市延安西路65号上海国际贵都大饭店办公楼405单元  
Phone: +86-21-62489820  
Fax: +86-21-62489821

© 2010 The Author(s). Licensee IntechOpen. This chapter is distributed under the terms of the [Creative Commons Attribution-NonCommercial-ShareAlike-3.0 License](https://creativecommons.org/licenses/by-nc-sa/3.0/), which permits use, distribution and reproduction for non-commercial purposes, provided the original is properly cited and derivative works building on this content are distributed under the same license.

IntechOpen

IntechOpen